

DOI 10.1070/RCR4428

Specific features of structure and properties of solutions, melts and solid states of polymers in confined nanometric volumes

A L Volynskii, A Yu Yarysheva, E G Rukhlya, L M Yarysheva, N F Bakeev

Department of Chemistry, M V Lomonosov Moscow State University
Leninskiye Gory 1, str. 3, 119991 Moscow, Russian Federation

The data on the influence of spatial restrictions on the structure and properties of polymers are analyzed. It is demonstrated that dispersion of polymers into aggregates of nanometre size critically changes all their characteristics in consequence of conformational restructuring of the polymeric chains. The spatial restrictions affect both characteristics of phase transitions in polymers (the crystallization and melting points, heat of melting and the degree of crystallinity decrease) and the processes of orientation of crystallites in asymmetric volumes of nanometre size. It is shown that these effects are primarily related to the changes in relative contribution of the stages of nucleation and growth of crystallite to the overall process occurring in confined volumes. Comparative analysis of the effects of spatial restrictions on the processes of crystallization of polymers and low-molecular-mass compounds is carried out. The similarity in changes in thermodynamic characteristics for both series of compounds is revealed.
The bibliography includes 211 references.

Contents

I. Introduction

Lately it has been shown [1–7] than transition from micro- to nanoscale volumes is accompanied by qualitative changes in physical, mechanical, physicochemical and other properties of compounds. Despite exceptional importance of information concerning properties of substances, and particularly, polymers, in the nano-sized state, it remains rather limited yet.

A L Volynskii Corresponding Member of the Russian Academy of Sciences, Professor, chief researcher of the Department of Chemistry, MSU. Telephone: (7 495) 939 55 09, e-mail: volynskii@mail.ru
A Yu Yarysheva Candidate of Chemical Sciences, Researcher of the same Deparment.
Telephone: (7 495) 939 55 09, e-mail: alyonusha@gmail.com
E G Rukhlya Candidate of Chemical Sciences, Senior researcher of the same Deparment. Telephone: (7 495) 939 11 82,
e-mail: katrin310@yandex.ru
L M Yarysheva Candidate of Chemical Sciences, Senior researcher of the same Deparment. Telephone: (7 495) 939 11 82,
e-mail: yarishev@gmail.com
N F Bakeev Academician, Professor of the same Department.
Telephon: (7-495) 332 58 46, e-mail: kbakeev@online.ru
Current research interests of the authors: structure and mechanics of polymers, physicochemical properties of polymers.

Received 25 September 2013
Uspekhi Khimii **83** (11) 1003 – 1026 (2014); translated by S E Boganov

Therefore it is not surprising that avalanche-like increase in the number of studies devoted to influence of spatial restrictions on the structure and properties of compounds has been observed in the recent years. Particularly, crystallization of polymers under applied two-dimensional restrictions attracts increasing interest.[8–14] Physical properties of crystalline polymers strongly depend on spatial restrictions under which the crystalline phase is formed. This fact has primary importance for production of small objects like nanorods and nanowire and development of novel devices for microelectronics, biomedicine and many other areas.[15–19] An impressive progress has been achieved in studies of influence of geometrical restriction on the structure and properties of amorphous polymers.[20]

The present review is devoted to generalization and analysis of experimental data demonstrating influence of volume restrictions on the rheological, mechanical, physicochemical, diffusion, thermodynamic and other properties of amorphous and crystalline polymers.

II. Specific features of structure and properties of surface layers and thin films of glassy polymers

In fact, volume restrictions imposed on condensed phases inevitably require consideration of the surface properties of these phases. Indeed, the decrease in the volumes of solids or liquids automatically leads to the increase in their specific surface areas, and grinding to the nanoscale size results in

complete transformation of the object into a surface layer. At the same time, it is known that superfine solid phases possess highly developed free surface, whose structure and properties fundamentally differ from the structure and properties of these phases in the bulk.

In the bulk of a solid or liquid, intermolecular interaction forces acting on a separate molecule from neighbouring molecules are, on average, mutually compensated. There is no this compensation on the surface, therefore some resultant force appears, which is directed to the bulk. If a molecule travels from the surface to the bulk, the intermolecular interaction forces execute a positive work. To translate a number of molecules from the bulk to the surface (*i.e.*, to increase the surface area), a positive work of external forces, which is proportional to the surface area change, has to be expended. It is the reason why a liquid droplet takes a spherical shape: the liquid behaves as if some forces contracting its surfaces acted tangentially to this surface. In other words, molecules in the surface layer are more attracted to each other than in the bulk due to the surface tension forces.

Surface tension forces make the surface like an elastic stretched film with the only difference that elastic forces in a film depend on its surface area (*i.e.*, on the film deformation), whereas the surface tension forces do not depend on the surface area. With a view to surface phenomena, there is no fundamental difference between properties of solids and liquids. A qualitative difference consists in that liquids can change their sizes and shapes under the action of surface tension forces, which makes it possible to detect these forces and, furthermore, to estimate some surface characteristics quantitatively. In the case of solids, surface forces also exist, but they are substantially smaller than the intermolecular interaction forces and, therefore, they are unable to change volume and shape of the solid. Nonetheless, the surface forces in solids determine a number of surface phenomena, which have been the subjects of extensive research for decades.[21,22]

Thus, the surface of liquids and solids represents some frame, which in analogy with the film mentioned above contracts enclosed volume to minimize itself.

II.1. Influence of nanometre volume restrictions on the glass transition temperature of amorphous polymers

The above outlined fundamental concepts concerning structure and properties of interfacial areas are of a general nature. All the more striking was the discovery of quite unusual behaviour of amorphous polymers in a glassy state made in the mid-1990s. It consists in depression in glass transition temperature (T_g) for thin films† and layers from tens to hundred nanometres thick. Using experimental methods reliably revealing the type of molecular movement in these thin films, quite specific effects were established. The obtained results turned out so unexpected and important that revision of many seemingly established concepts concerning polymer structure and properties is required.

The first systematic study dealing with precision measurement of T_g in thin films of a glassy polymer was published in 1994.[23] In this study, T_g of thin polystyrene (PS) films applied on a silicon wafer passivated by hydrogen

† Recall that thin films are the films with thickness from 100 to 500 nm, ultrathin films are of thickness from 10 to 100 nm; films < 10 nm thick are considered as monolayers.

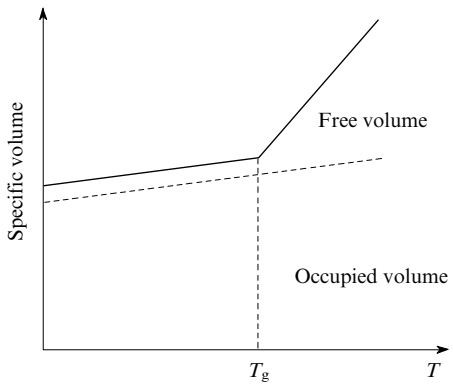

Figure 1. Temperature dependence of the specific volume for a linear amorphous polymer.[24]

was measured with the use of ellipsometry. Ellipsometry makes it possible to determine the polymer film thickness with high precision. Moreover, dependence of a film thickness on temperature can be obtained. In fact, this is equivalent to determination of thermal expansion coefficient of the polymer,[24] which is abruptly changed at the point of its glass transition (Fig. 1).

Upon measuring the temperature dependence of the film thickness, one determines the polymer T_g value by the jump of thermal expansion coefficient. This method was considered in detail by Sharpl *et al.*[25] At present, ellipsometry is one of most widely used techniques for estimation of T_g of thin polymer films, both free and applied on wafers.

Keddie *et al.*[23] measured film thicknesses from 300 to 10 nm. Evidently, they were the first to show that starting from thickness of 40 nm, the glass transition temperature of PS dramatically decreases in comparison with T_g of bulky polymer. For a 10 nm thick film, the depression was 25 K that is beyond the experimental error of determination of T_g by ellipsometry. The average molecular mass (M_w) of polystyrene used in this study was $(120-2900)\times10^3$, while polymer coil sizes varied from 20 to 100 nm. No correlation between T_g and M_w was observed, while the obtained data were well described by the relation

$$T_g = T_g^{bloc}\left[1-\left(\frac{a}{h}\right)^{\delta}\right]$$

where T_g^{bloc} is the glass transition temperature of PS in the bulk, h is the film thickness, $a = 3.2$ nm, $\delta = 1.8$.

Later on, a large number of studies devoted to this subject was published. In particular, methods for producing and investigation of properties of thin polymer films on solid substrates and free thin films of amorphous polymers were developed. In contrast to the surface layers of low-molecular-mass solids, in the surface layers of glassy polymers, molecules are not drawn to each other, but form a thin layer with large free volume as indicated by depression of T_g.

II.2. The glass transition temperature of thin films of glassy polymers on solid wafers

The progress of studies of glass transition temperatures of thin films of glassy polymers applied on solid wafers was accompanied by extension of both research techniques and objects of the studies. Thin films of classical amorphous

polymers such as PS, polymethyl methacrylate (PMMA) and so on were used in most of the studies. One surface of these films was in contact with a solid substrate, and the other contacted with air; polymer T_g was measured for the polymer/air interface.

To estimate T_g, Schwab *et al.*[26] used measurements of the birefringence relaxation for ultrathin PS films on glass substrates. It was shown that the glass transition temperature decreased by 15–20 °C when film thickness decreased from 10 μm to 5.8 nm. In thick films (>10 μm), molecules located close to the polymer/air interface underwent relaxation faster than other molecules. Dynamics of relaxation of ultrathin (<40 nm) PS films was investigated using photon correlation spectroscopy in combination with quartz crystal microbalance techniques.[27] It was found that T_g in these films was more than 70 °C lower than in the bulk. The shapes of the relaxation function and the temperature dependence of relaxation time above T_g were analogous to those of the bulk polymer, though shifted along the temperature axis by ~70 °C. Similar results were obtained by Wolff and Johannsmann[28] in measurements of high-frequency shear compliance in ultrathin (10 and 93 nm) PS films on quartz wafers with the use of quartz crystal resonators. It was revealed that reduction of shear compliance takes place for films with thickness of ⩾10 nm, whereas for films of <10 nm the shear compliance increases by more than 50%. It was assumed that these effects are due to geometrical restrictions leading to parachute-like conformations of the polymer chains.

The use of positron annihilation technique turned out to be efficient in the studies of free volume in thin films.[29] Positron annihilation lifetime and Doppler broadening of annihilation radiation were measured for PS films using the mono-energetic slow positron probe.[30,31] Strong changes for a signal of positron annihilation were observed at a small (20 nm) distance from the sample surface. The orthopositronium lifetime in the polymer increased nearby the surface, whereas its intensity decreased. The results of lifetime measurements were interpreted as an expansion of local free-volume holes nearby the surface. Distribution of free volume and the holes near the surface was found to be broader than in the bulk. Spectra of positron annihilation lifetime for positrons with energies of 0.2–3.0 keV were recorded for epoxy polymer using an electrotechnical laboratory slow-positron device.[32] It was shown that the orthopositronium lifetime, increased in the bulk, while decreased near the surface. This technique makes it possible to determine the fraction of free volume in polymer (f_v) using the principle of time–temperature superposition[33]

$$f_v = f_m + (T - T_g)\Delta\alpha$$

where f_m is the fraction of free volume at T_g, T is the temperature at which the experiment is carried out, $\Delta\alpha$ is the difference of coefficients of thermal expansion above and below T_g. It was shown that in the near-surface layer, the size of free-volume holes increases, as well as their fraction in the volume increases up to 4%, while T_g decreases from 50 to 10 °C.

Similar changes were revealed for polyethylene terephthalate (PETP), which is capable of crystallization in contrast to PS. To obtain T_g in thin films of PETP, ellipsometry was used.[34] It was demonstrated that T_g in this case strongly depends on the remoteness of the layer from the polymer/air interface. For example, T_g in the bulk is equal to 71 °C, whereas it is equal to 65 and 56 °C at the depth of 25 nm and 15 nm, respectively.

The fact that there is the T_g gradient in near-surface layers was confirmed by the results of several studies,[36–38] which were analyzed in a review by Alcoutlabi and McKenna.[35] A method for synthesis of PS containing pyrene fluorescent label was described in these studies. Thin film of labelled PS was applied on a PS film containing no label. Thicknesses and relative positions of PS layers with and without the label were varied. The local T_g value for thin films of labelled PS depending on their thickness and location in the multilayer system was measured using fluorescence analysis. It was found that the glass transition temperature of the labelled PS layer applied on the surface of a thick (270 nm) PS film strongly decreases with its thickening. The glass transition temperature of a thin (14 nm) PS layer with a fluorescent label (T_{gf}) changes non-monotonically depending on its location in the multilayer system. If this layer is covered by a PS layer of a thickness of >18–30 nm without a label, its T_{gf} is equal to T_g of PS in the bulk. For smaller thicknesses of the covering PS layer, T_{gf} decreases in comparison with T_g of the bulk. The difference between these temperatures increases with thinning of the covering layer. The authors concluded that the strongest perturbation resulting in the depression in the glass transition temperature occurs in the polymer surface layers. At the same time, the layers adjoining the perturbed layer are also changed, and these changes determine the difference in molecular movement in these layers and in the bulk of the polymer. In other words, there is not merely surface thin layer, but some gradient in the polymer structure directed from the surface to the bulk and associated with depression in T_g at the surface as compared with T_g in the polymer bulk. The authors suppose that a two- or three-layer model can be used to describe this phenomenon. The effect of depression in T_g of the surface layer is confirmed by the data obtained in the study of interaction of metal nanoparticles with the surface of a glassy polymer.[25]

An important information on the structure and properties of surface layers in polymers can be obtained with the use of various types of probe microscopy. In particular, surface molecular movement in monodisperse PS was characterized using lateral force microscopy, scanning viscoelasticity microscopy and differential X-ray photoelectron spectroscopy.[39] It was demonstrated that the molecular movement is more intensive in the surface layer than in the bulk. Forced modulation scanning force microscopy and lateral force microscopy were applied to an analysis of surface molecular movement in monodisperse PS in another study.[40] Modulation scanning force microscopy makes it possible to determine the dynamic shear modulus (E') and the tangent of the phase shift angle ($\tan\varphi$) in surface layers. It was found that in the case of polymer with $M_w < 2.6 \times 10^4$, the E' value near the surface is lower, and $\tan\varphi$ is greater than in the bulk. The glass transition temperature of PS at the polymer/air interface is below room temperature (Fig. 2).

The T_g depression in thin films is also observed for mixtures of compatible polymers. Dependences of T_g on the film thickness and composition of compatible mixtures of poly(2,6-dimethyl-1,4-phenylene oxide) (PPO) and PS were obtained.[42] Thin films were produced by evaporation of toluene from solutions of the polymers applied on a silicone substrate. Ellipsometry was used to measure T_g. It was

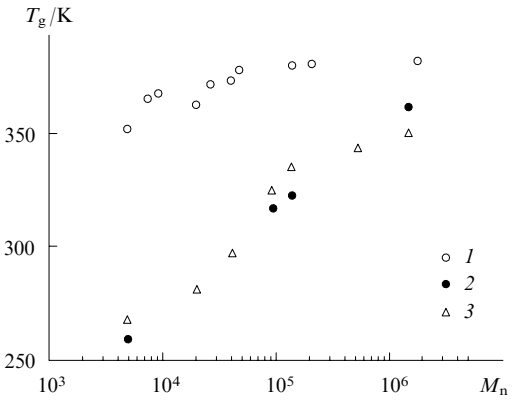

Figure 2. Polystyrene glass transition temperature in the bulk (*1*) and on the surface (*2*, *3*) *vs.* number-average molecular mass.[41] The T_g values are obtained by differential scanning calorimetry (*1*), and lateral force (*2*) and scanning viscoelasticity microscopy (*3*).

demonstrated that the composition of polymer mixtures affects T_g of thin films like it does in the case of bulky polymers; however, depression in T_g with decreasing film thickness was observed for all compositions (Fig. 3).

In the case of thin films on wafers, the nature of interfacial contact strongly affects the intensity of molecular movement.[43] This influence was clearly ascertained, *e.g.*, in the study of electron densities in surface layers of thin films of PS, PMMA and poly(4-vinylpyridine) (P4VP) on SiO_2 wafers using X-ray reflectometry.[44] The film thickness was $\sim 4\,R_g$, where R_g is the gyration radius of macromolecule. It was found that electron density near the free film surface decreases for PS and PMMA and increases for P4VP. In authors' opinion, it is caused by different strength of interactions of hydrophobic (PS and PMMA) and hydrophilic (P4VP) polymers with the polar substrate.

Significant influence of the substrate nature on the molecular mobility of a polymer in the layer adjacent to it was revealed in the study of mobility of PS chains, which were labelled at the ends with fluorescent labels, in the films applied on a quartz substrate.[45] Using fluorescence spectroscopy, macromolecule diffusion constant (D) was measured. It was found that D decreases at the film thickness of < 150 nm. In agreement with the inference drawn in another study,[46] the observed changes in the D values were attributed to the strong interaction of the polymer with the substrate, which restricts the molecular mobility of polymer chains.

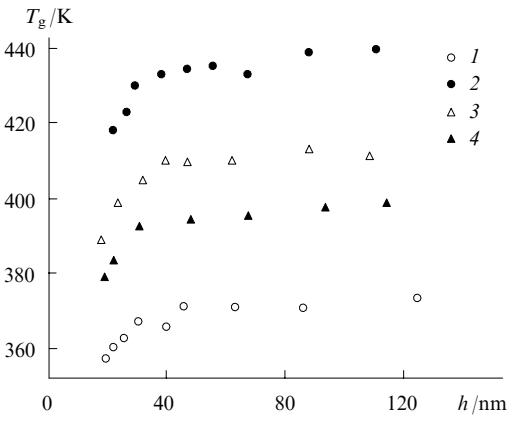

Figure 3. Glass transition temperature of pure PS (*1*) and its mixtures with PPO (*2*–*4*) *vs.* film thickness (h).[42] PPO : PS ratios = 7 : 3 (*2*), 5 : 5 (*3*), 3 : 7 (*4*).

An analogous conclusion was made from measurements of T_g in thin films of PS of various molecular masses as a function of their thicknesses using Brillouin scattering and ellipsometry.[47] Comparison of the results obtained for free films and films on silicon oxide substrates was carried out. It was shown that strong depression (by more than 60 °C) in T_g for free films is observed if their thickness is smaller than the size of unperturbed macromolecular coil. In the case of films on substrates, depression in T_g, was also observed, but it was equal to 4 °C only. Extremely strong influence of the wafer on the thermal expansion coefficient of thin films of deuterated PS was revealed using neutron scattering.[48] It appeared that there is a substantial gradient of thermal expansion coefficient of deuterated PS across the film thickness, this gradient depends on the nature of interfacial contact. This effect was also explained by interaction of the polymer with the substrate.

The influence of interfacial energy on T_g of thin (18 – 80 nm) films of PS and PMMA was demonstrated by Fryer *et al.*[49] Polymer films were applied on a silicon substrate; T_g was measured using three techniques; local thermal analysis, ellipsometry and X-ray reflectometry, which gave similar results. It was ascertained for films of different thickness that decrease in T_g depends linearly on the interfacial energy.

The study of relaxation of optical birefringence made it possible to estimate T_g of ultrathin PS films on glass substrates.[26] It was demonstrated that T_g decreased by 15 – 20 degrees with the decrease in the film thickness from 10 μm to 5.8 nm. In thick films (> 10 μm), molecules located close to the polymer/air interface relax faster than those being in contact with the substrate. Significant restrictions on molecular mobility in thin PS films on a silicon wafer were also revealed,[50] although the thicknesses of the films under study were much larger than the gyration radius of the macromolecule. It was supposed that the found molecular mobility restrictions arose from strong interaction of the polymer with the substrate. The electron density gradient in the direction normal to the plane of thin (20 – 80 nm) films of isotactic PMMA on a silicon wafer was determined with the use of X-ray reflectometry.[51] This method is suitable for estimating slight density fluctuations. It was shown that in the polymer being in contact with the substrate, the electron density increases independently of the polymer tacticity or film thickness. This effect was explained by more dense packing of macromolecules at the interface due to interfacial interaction and selective adsorption of stereoregular chains.

Dynamics of isotactic PMMA in the temperature range 273 – 392 K was studied using dielectric relaxation spectroscopy.[52] There were two peaks of dielectric losses corresponding to the α- and β-transitions. It was found that the β-transition is independent of the film thickness, while the α-transition is dependent and substantially decreases with its decrease. According to ellipsometry data, T_g of the polymer contacting with a silica substrate gradually increased with decreasing thickness. In authors' opinion, this indicates strong interaction of the polymer with the substrate.

The calculation showed [53] that T_g at the free surface of a polymer is always lower than T_g in the bulk. However, the glass transition temperature of a thin film on a solid substrate can increase. Simultaneously, T_g of a polymer is affected by the substrate surface topography. It was shown [54 – 56] that the macromolecule dynamics can become slower (T_g increases) even if there is no strong interaction between polymer and substrate, but a polymer particle (the polymer phase) is situated in a 'cage' (a nanometre-sized cavity) on the substrate surface.

Adsorption effects at the interface leading to restrictions on mobility of polymer chains can be so strong that cause the increase in T_g of a polymer. Modulated differential scanning calorimetry was used to probe the behaviour of PMMA adsorbed on a silica substrate.[57] It was found that T_g of adsorbed PMMA grew from 108 (T_g of bulk polymer) to 136 °C.

II.3. The glass transition temperature of free thin films of glassy polymers

As noted above, interaction of a polymer with the substrate can significantly influence molecular movement in thin polymer films. At the same time, there are methods making it possible to prepare free films of a few tens of nanometres thick, as well as methods for measurement of their T_g.[58] The films can be prepared by two methods:

— having prepared a film on a substrate, to float it on a water surface and then to place it on a supporting net;

— to evaporate solvent from a thin layer of a polymer solution applied onto a more dense liquid, usually, water;‡ to place the formed film in a special holder to study its properties.

Most of studies of free films were carried out for polystyrene, thus making it possible to summarize the experimental data in a single figure (Fig. 4).[59] It appears that depression in T_g is much stronger in this case than in the case of films on solid substrates. Furthermore, the dependence of T_g of free PS films on the film thickness is not only much more pronounced, but also qualitatively different. There are two types of these dependences. If molecular mass is relatively low, the dependence of T_g on the film thickness resembles that typical of PS films on substrates: T_g gradually decreases, starting from a thickness of 50 – 70 nm, and does not depend on the molecular mass. However, the latter dependence clearly reveals itself for PS of higher molecular mass: T_g starts to depend linearly on the molecular mass, and, at some film thickness, it starts to decrease sharply. The higher the polymer molecular mass, the sharper the depression in T_g with decreasing the film thickness (in the case of high molecular masses, T_g begins to decrease at a lower film thickness).

Thus, similarly to the case of films on substrates, in the case of free films, a substantial decrease of T_g relative to the bulk value is observed; this decrease depends on polymer molecular mass and is much greater than for films on substrates.

It is noteworthy that sharp lowering of mechanical characteristics in surface layers and thin films of glassy polymers is confirmed by measurements of their modulus of elasticity (E). In a series of studies,[60 – 63] an approach based on the analysis of surface microrelief formed upon deformation of two-layer polymer systems [64, 65] was used to estimate the modulus of elasticity of polymer films. The results are shown in Fig. 5. It is clear that the modulus of elasticity sharply decreases (4 – 5-fold) irrespective of the polymer molecular mass when PS film thickness becomes $< 50 – 70$ nm in full agreement with the above discussed results of measurements of T_g in thin films of glassy polymers (*cf.* Figs 4 and 5).

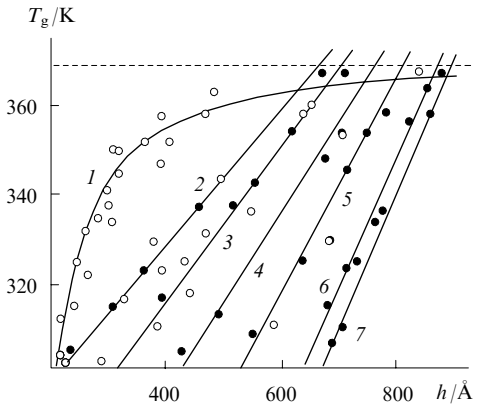

Figure 4. Glass transition temperature of free PS-films *vs.* their thickness according to the data of ellipsometry (bright circles) and Brillouin light scattering (dark circles).[59]
$M_w \times 10^{-3}$: 116 – 347 (*1*), 541 (*2*), 691 (*3*), 1250 (*4*), 2077 (*5*), 6700 (*6*), 9000 (*7*). Dashed line indicates the glass transition temperature of bulk PS.

Summarizing the available data on T_g of nanometre polymer layers, it is important to note that the glass transition temperature of free films usually decreases as compared to the bulk value, with the depression degree depending on the polymer molecular mass (apart from the results of the above considered studies, this fact was also corroborated by the data of other studies [53, 66 – 68]). If the film surface is in contact with other surfaces, the T_g shift depends on the type of interaction. Sufficiently strong interaction between polymer and substrate may result in invariance or even in an increase in T_g of thin films.[57, 67 – 69] Obviously, the latter effect is caused by adsorption of a polymer on the interface, strongly decelerating the motion of polymer chains. At present, there is no quantitative

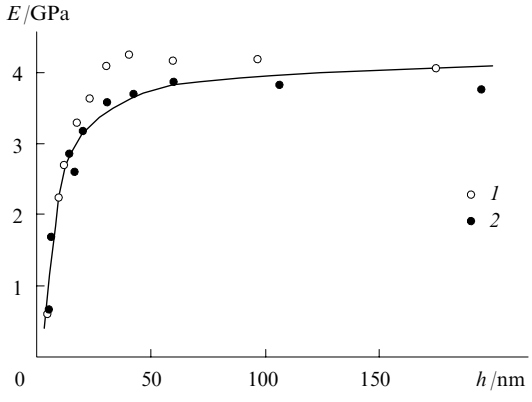

Figure 5. Modulus of elasticity *vs.* PS film thickness.[63]
$M_w \times 10^{-3}$: 1800 (*1*), 114 (*2*).

‡ In fact, this methodology is the methodology of producing supporting film wafers for transmission electron microscopy.

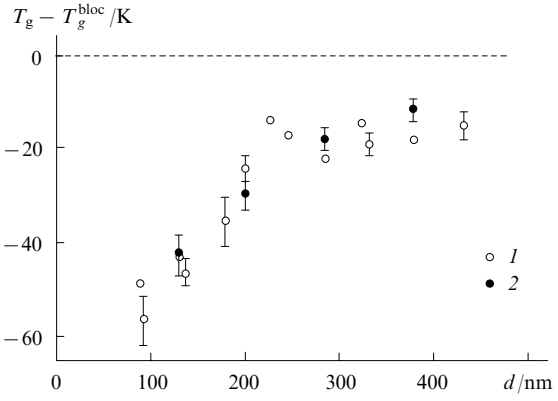

Figure 6. Depression in glass transition temperature ($T_g - T_g^{bloc}$) for PS spherical nanoparticles of various diameters (d).[70] The T_g and T_g^{bloc} values were obtained using differential scanning calorimetry (*1*) or dilatometry (*2*); dashed line corresponds to T_g of bulk PS.

theory able to describe in full the depression in T_g for thin films of amorphous polymers, which was observed by Keddie *et al.*[23] for the first time. It was suggested[35] that the reason for this situation consists in insufficient knowledge of both this particular phenomenon, and the overall mechanism of glass transition in polymers.

It is important to note that the effect of the decrease in T_g of a polymer with the decrease in its volume, which was found by Keddie *et al.*,[23] is observed not only for films and surface layers of amorphous polymers. A procedure of preparation of nanometre-sized spherical PS particles by emulsion polymerization under special conditions was reported.[70] This procedure makes it possible to prepare an ensemble of nanoparticles with sizes from 100 to 500 nm. It was found that T_g depression is clearly observed for these particles as well (Fig. 6).

Thus, the effect of depression in T_g for thin films and surface nanometre-sized layers of amorphous polymers really exists; the undistorted effect can be observed only for free surfaces not contacting with a solid substrate.

II.4. Possible causes of depression in glass transition temperature for thin films and surface layers of amorphous polymers

As shown above, a substantial decrease in T_g is observed and the overall molecular mobility (α-relaxation) becomes easier in free thin films, as well as often in thin films applied on substrates. Naturally, much attention was paid to establishing the mechanism of this phenomenon. However, there is no single point of view on this mechanism to date.

One of approaches to solve this problem is based on consideration of specific features of glass transition in a polymer in a confined volume (it comes to the situation when the polymer phase is so small that realization of equilibrium chain conformations is hampered and the character of overall molecular movement is changed). It is known[71] that the glass transition is caused by cooperative molecular movement, which is possible only in a sufficiently vast polymer phase. The optical second-harmonic generation technique was used to measure molecular mobility in surface layers of low-molecular-mass glass-forming liquids.[72] It was found that the collective dynamics of the molecular motion in surface layers is broken (its intensity increases as compared to that in the bulk), resulting in formation of a glassy state.

A substantial intensification of molecular motion in surface layers in a polymer was demonstrated when the specifics of molecular motion in poly(4-methylstyrene), PS and poly(*p-tert*-butylstyrene) were studied using X-ray photoelectron spectroscopy.[73] It was found that the surface activation energy of solid polymer diffusion at room temperature (92 kJ mol^{-1}) is much lower than the activation energy of self-diffusion in the PS melt at much higher temperature of 170–190 °C (167.6 kJ mol^{-1}). Obviously, this fact testifies to decrease of the scale of the molecular motion, reflecting changes in the collective dynamics in the polymer surface layer as compared to the polymer bulk. Using local thermal analysis, T_g of thin films of PS and PMMA on SiO_2 wafers treated with hexamethyldisilazane (HMDS) were determined.[74] The glass transition temperature of PMMA appeared to increase when it was applied on polar SiO_2 wafers and to decrease if it was applied on non-polar SiO_2–HMDS wafers. A decrease in T_g of PS films was observed for both wafer types.

In the case of amorphous polymers, the collective dynamics is disturbed if the polymer phase thickness is smaller than mean-square distance between the chain ends. It results in the decrease in the size of a devitrifying part of the chain, and consequently, in the depression in glass transition temperature. The dependence of the glass transition temperature of films of PS with $M_w = 767 \times 10^3$ and 2240×10^3 on their thicknesses is presented in Fig. 7. As can be seen, the beginning of T_g decrease correlates to a certain degree with unperturbed sizes of macromolecule coils.

The influence of volume restrictions on the type of molecular motion of polymer chains is also corroborated by some theoretical studies. A model of interactions was suggested,[75] with the use of which it was shown that T_g sharply decreases if the thickness of a free film is smaller than the distance between the ends of unperturbed macromolecular chain. It is supposed that this is the reason for the strong dependence of T_g of thin polymer films on the molecular mass. It is thought that in free films of polymers with high molecular mass, first, a planar orientation of the polymer chains is induced (the distance between the ends of an unperturbed chain becomes comparable with the film

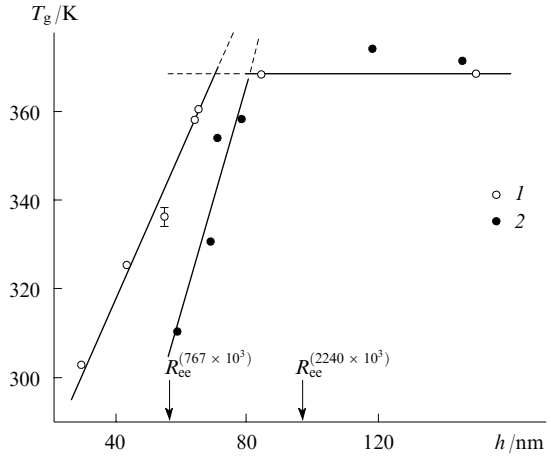

Figure 7. Glass transition temperatures of free films of PS with $M_w \times 10^{-3} = 767$ (*1*) and 2240 (*2*) *vs.* their thickness.[47] Unperturbed coil sizes (R_{ee}) are marked with arrows.

thickness in this case), and, second, the cooperative lengths of chain segments nearby the surface are reduced. As a result, the scale of local segmental movements of molecular units decreases near the interfacial surface. In particular, the T_g decrease is attributed to the decrease in the interaction parameter. The T_g values calculated according to this model are in good agreement with experimental data.

Monte Carlo simulations have been applied to the study of molecular mobility in free films depending on their thickness and to the analysis of macromolecule conformations depending on the distance from the interface, and also diffusion coefficient for linear and cyclic molecule was computed in addition.[76] It was found that T_g decreases with decreasing film thickness. In free films, conformations are considerably more compact than in the case of Gaussian distribution. All of the effects are less pronounced for cyclic molecules than for linear ones, although in both cases, the theory predicts existence of a liquid-like interface layer where molecular mobility is significantly higher than in the bulk. Analogous conclusions were drawn from another theoretical study using molecular dynamics calculations,[77] which showed that the mobility of amorphous polyethylene (PE) molecules increases, while the density decreases in the direction from the bulk to the surface. De Gennes[78] suggested an idea about possible existence of sliding motion of polymer chains in confined volumes. According to calculations, the glass transition temperature in this case should decrease if geometrical size of the polymer phase is comparable with the sizes of unperturbed molecules.

Another point of view connecting the decrease in T_g in surface layers with segregation of terminal groups of macromolecules in these layers is no less popular.[39–42] The concept of segregation of terminal groups at interfaces is based on the fact that, according to the Flory–Fox theory,[79] the chain ends are in essence plasticizers depressing T_g. As supposed, the increase in the concentration of terminal groups in the surface layers of polymers in comparison with the bulk results in the increase in the free volume, and, hence, in the decrease in T_g. To prove this assumption, deuterated PS with protonated terminal groups was studied using dynamic secondary ion mass spectrometry.[39] The concentration profile of terminal hydrogen-containing groups in the direction normal to the film surface was obtained. An increase in the concentration of these groups in the surface layer relative to the concentration of deuterated groups was revealed in support of the hypothesis of increase in the concentration of terminal groups in this layer.

To ascertain the mechanism of T_g depression in surface layers and thin films of amorphous polymers, three samples of PS with different terminal groups (conventional PS, as well as PS2 and PS3 with NH_2 and COOH end groups, respectively) were synthesized and a large number of monodisperse fractions of these samples were obtained by Satomi *et al.*[80] To elucidate the effect of terminal groups and cooperative length of vitrifying elements of the structure on surface depression in T_g, which was determined using atomic force and scanning viscoelasticity microscopies making it possible to obtain dynamic characteristics of polymer surface layers, the polymer molecular mass and the nature of terminal groups was varied. With the use of X-ray photoelectron spectroscopy, concentration of the terminal groups at the surface was estimated. It was found that the effect of T_g decrease depending on the molecular mass is observed both in the bulk and at surface, with surface T_g depression relative to bulk T_g being observed in the whole molecular mass range used. Surface T_g starts to decrease at lower molecular masses and, depending on the latter, decreases faster than bulk T_g. The exception was PS with terminal COOH groups, which did not exhibit any dependence of the decrease in T_g on molecular masses. With the use of the time–temperature superposition principle, effective activation energies of α-relaxation were obtained. It was demonstrated that the activation energy of α-transition in the surface layer is 230 ± 10 kJ mol^{-1} in all the cases, while this value in the bulk ranges from 360 to 880 kJ mol^{-1} according to different data.[81] The results of this study indicate that both of the considered factors may affect the T_g depression at polymer surfaces.

A three-layer model was suggested in some studies (see, *e.g.*, Refs 82–84) to describe T_g depression in thin polymer layers. Each of the layers was characterized by its own dynamics. Molecular mobility was assumed to be higher near the free surface than in the bulk, whereas in the centre it was taken to be equal to that in the bulk, and it was thought to be restricted at the interface as compared wth that in the bulk. The results obtained using this model were in good agreement with the experimental data. It is important to note that T_g in surface layers decreases only in the case of glassy polymers. An analogous effect was also observed for the amorphous component of crystalline high-density polyethylene.[85]

It should be noted in conclusion that the effect of significant depression in T_g of thin films of amorphous polymers, which was revealed in the mid-1990s, represent a fundamental property of these films. This phenomenon was not noticed earlier since the contribution of surface layers to the characteristics of bulky polymers studied before is negligible and was not taken into account. However, if deformation results in development of a high interface level, this contribution should be considered.

Development of a high interface level is typical of one of the fundamental types of inelastic deformation of solid polymers, *viz.*, of crazing.[86–88] The most important feature of polymer crazing consists in that the development of this type of plastic strain is accompanied by emergence and growth of specific areas called crazes, which include oriented polymer. A TEM image of a single craze in a deformed thin film of PS is shown in Fig. 8.[88]

The craze is seen as a kind of discontinuity in the polymer. A feature of the craze structure consists in that the blocks of initial (unstrained) material are connected by separated thinnest fibrils of oriented polymer. Diameters of the fibrils and distances between them range from a few to tens of nanometres. Obviously, such a small size of macromolecule aggregates should influence their properties.

The first systematic study of mechanical properties of crazes of polycarbonate (PC) was carried out by Kambour and Kopp,[89] who obtained individual crazes by deformation of glassy PC in an active liquid (ethanol). Using a special device, the authors measured the changes in the distance between the edges of an individual craze depending on the force applied to the sample ends. The thus obtained stretching dependences for a single craze had a characteristic shape (Fig. 9). As can be seen, the yield stress of the craze material is considerably lower than that of the starting bulky polymer.

After several consecutive cycles of deformation–relaxation, it was revealed that the initial modulus of elasticity and the yield stress decreased with increasing width of the

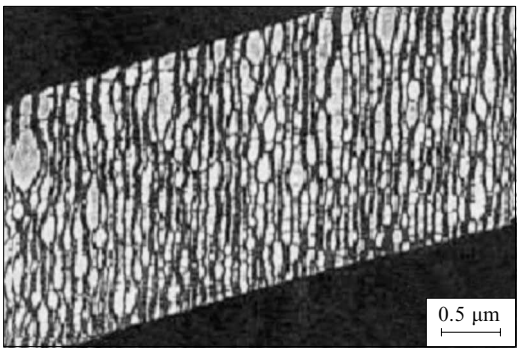

Figure 8. TEM image of a single craze in a strained (stretching axis is vertical) thin film of PS.[88]

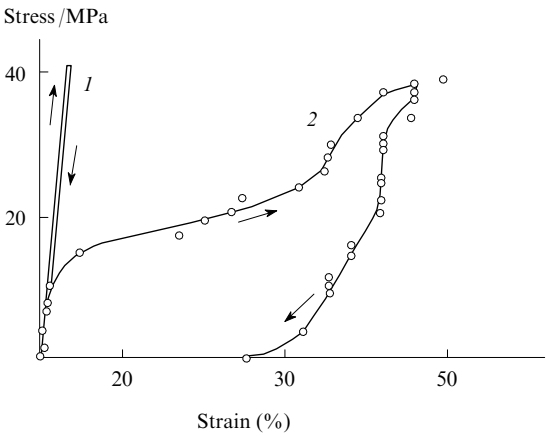

Figure 9. Plots of stretching and shrinkage at constant velocity for PC (*1*) and a single craze in PC (*2*).[89]

starting craze. The modulus of elasticity was ~ 4 times lower than that of unstressed polymer. It was also shown in the same study that 'dry' crazes of PC deformed by 50%–60% are able to restore their sizes spontaneously after removing the load. It is noteworthy that this behaviour is untypical of glassy polymers oriented by cold drawing. As can be seen, the mechanical properties of the fine material of a single craze cardinally differ from those of the bulky polymer. As follows from the above data, dispersion of a glassy polymer into nanometre-sized aggregates of macromolecules has an effect on its mechanical behaviour. First of all, this effect manifests itself in the increase in the polymer compliance and emergence of a possibility of large reversible deformations, which are untypical of the glassy state. The strain-induced softening of amorphous and crystalline polymers was considered in detail.[90] It was shown that this effect is general in nature and represents a fundamental feature of solid polymers.

III. Specifics of mass transfer for polymers in confined volumes

The experimental data discussed above indicate complex influence of spatial restrictions on the structure and properties of polymers. Polymer films, including the films of nanometre thickness, are formed by isolation of polymers from solutions or by solidification of their melts. Obviously, the unusual properties of polymers in nanometre volumes are introduced at early stages of their formation, *i.e.*, in solutions or melts. In this connection, studies of effects of nanometre volume restrictions on specifics of mass transfer during their flow and diffusion are topical. Methodologically, such studies represent a serious problem since it is necessary to investigate mass transfer processes in extremely narrow spaces (pores), whose sizes and geometry are difficult to control.

Practical approaches to preparation of suitable objects are opened by recently developed methods for production of porous aluminium plates,[91,92] in which the pore diameter can be varied in wide ranges, keeping intact their cylindrical shape. SEM images of two porous membranes with pores of 200 and 80 nm in diameter are shown in Fig. 10.

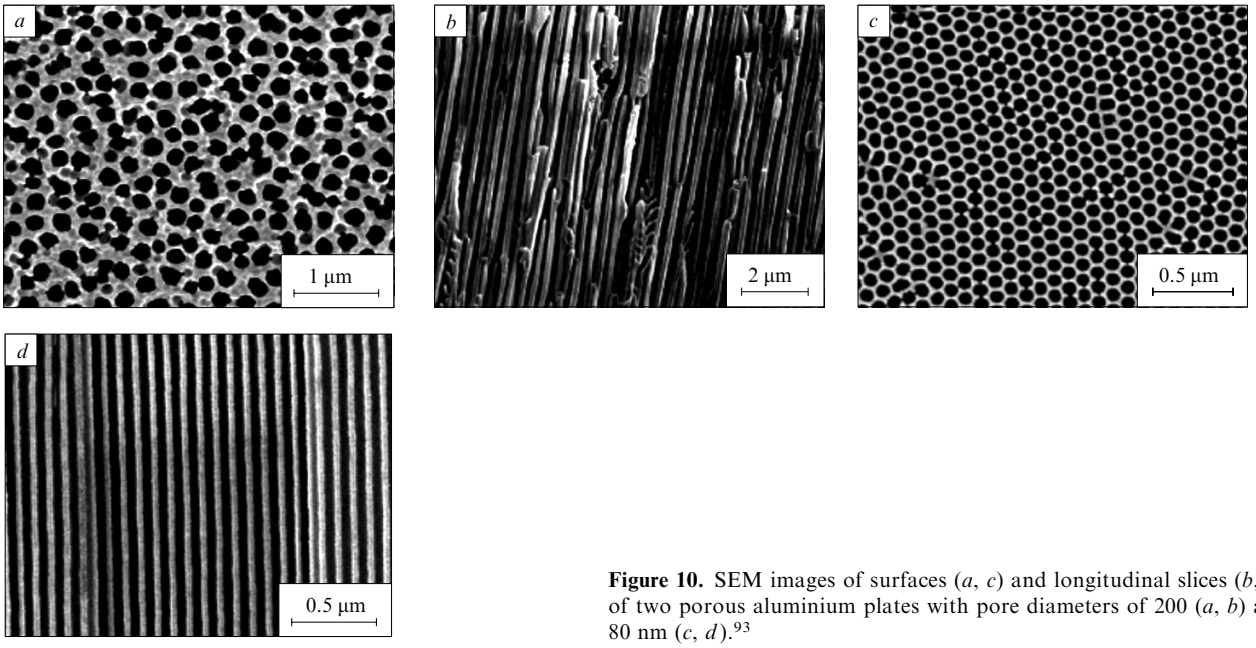

Figure 10. SEM images of surfaces (*a*, *c*) and longitudinal slices (*b*, *d*) of two porous aluminium plates with pore diameters of 200 (*a*, *b*) and 80 nm (*c*, *d*).[93]

III.1. Phase mass transfer in confined volumes of polymers

Using aluminium plates with nanometre-sized cylindrical pores, one can study the mass transfer processes in solutions or in melts in channels with volume restrictions at the nanoscale. The key specific feature of polymers consists in that the volume restrictions have to affect the chain conformations. Indeed, *e.g.*, if the film thickness is smaller than the Gaussian coil size, the conformation of this coil has to be changed inevitably. Such a change was really revealed [94]. It was unexpectedly found that the coil size decreased only in the direction normal to the side surface of the cylindrical nanopore, while the size in the direction of the nanopore axis remained invariable and equal to the coil size in the bulk. In other words, the chain penetrating into a cylindrical pore is compressed in the direction normal to the pore axis, but remains unperturbed along this axis even when pore sizes and molecular masses of macromolecules were varied in wide ranges.

The diagram of conformational changes of a macromolecule situated in a pore with a diameter smaller than the radius of gyration of the macromolecule coil is shown in Fig. 11. It reproduces the results obtained in the studies of conventional and deuterated PSs with the use of small-angle neutron scattering.[94, 96] This unique phenomenon is considered to be caused by changes in interpenetration of polymer chains. Assuming incompressibility of polymer chains under the applied spatial restrictions, interpenetration along the pore axis can be considered as decreasing since the polymer chains are restricted in the radial direction. By this we mean that interpenetration of chains should decrease with the increase in the polymer molecular mass, whereby the chains could preserve unperturbed conformations along the axial direction.

This situation is analogous to the situation taking place upon crazing of polymers.[86 – 88] Recall that crazing is in fact dispersing a polymer into aggregates of nanometre size, which consist of oriented chains (Fig. 12). Formation of these aggregates is analogous to formation of the polymer structure filling a nanometre-sized cylindrical pore (see Fig. 11). At the same time, when fibrillar aggregates of macromolecules are formed in the structure of a craze, some entanglements available in the polymer before crazing are necessarily lost due to geometrical requirements. The process of development of nanometre-sized pores in the structure of a strained polymer is sketched in Fig. 13. It was demonstrated theoretically and experimentally [98] that during polymer crazing, disentanglement or scission of entanglement network should occur.

Two different phenomena are considered in the literature: penetration of a polymer melt into nanometre-sized pores under the action of an external force and formation of nanometre-sized aggregates of macromolecules in the craze structure also under the action of an external force. The difference between these phenomena consists in that there are rigid walls in the first case (at flow of a melt) and there are no such walls in the second case (at crazing). However, these phenomena have very important resemblance: continuous entanglement network of polymer macromolecules is dispersed into nanometre-sized aggregates. It is difficult to imagine this process without loss (disentanglement or scission) of at least a part of entanglements. Therefore it is not

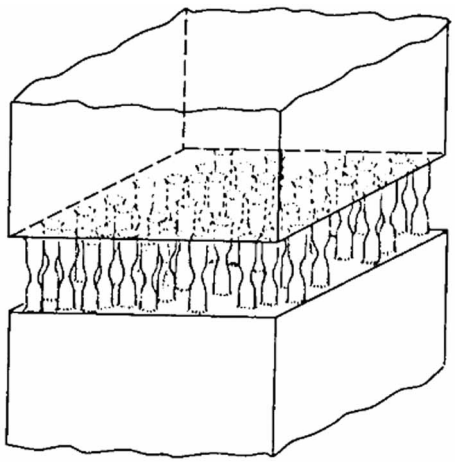

Figure 12. Diagram of a craze structure.[87]
The stretching axis is vertical.

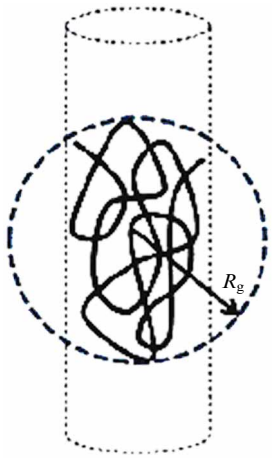

Figure 11. Diagram of conformational changes of a macromolecule during its penetration in a nanopore with a diameter smaller than the macromolecule gyration radius (R_g).[95]

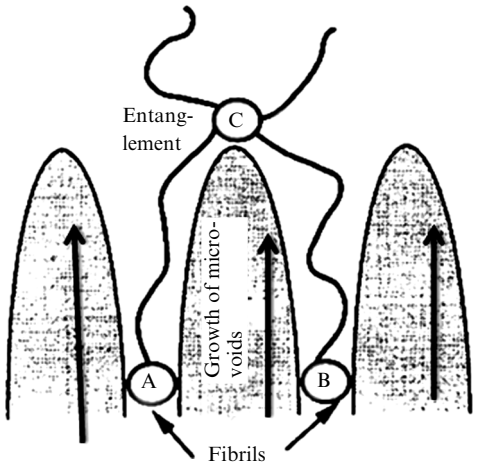

Figure 13. Diagram of invasion of a nanometre-sized pore to the polymer bulk during crazing.[97]
A separate chain situated on the way of growing pore is shown. This chain has to be disentangled or destroyed to open way for further growth of the pore.

surprizing that the authors who studied these phenomena came to a similar conclusion: interpenetration of macromolecules decreases in the first case, and a portion of entanglements is lost in the second case.

For a fibrillar-porous structure of a craze to arise, it is necessary that a part of entanglements in the initial bulky polymer, which are in the path of a developing nanopore, should be either disentangled or scissored. If not, formation of highly developed surface typical of the craze structure is impossible.

This conclusion unequivocally follows from the experimental results of a study,[99] where the dependence of strain necessary to initiate crazing in unannealed samples of PS and those annealed at 130 °C for 10 min on the strain temperature was obtained. After annealing, no craze was observed using optical microscope. It is clearly seen (Fig. 14) that the repeated initiation of crazing occurs at considerably lower strains irrespective of the temperature of stretching of PS.[99] However, restoring the optical transparency of the polymer upon annealing does not testify to complete curing of interfaces, which should be accompanied by restoring the polymer characteristics. This effect is connected with the geometrical requirements to lose a part of entanglements at crazing, as it was noted above. Glassy polymer is a conglomerate of entangled macromolecules, which are linked by a system of physical knots. Under deformation, chain conformations are changed, and the knots shift relative to each other without visible destruction. Existence of these steady knots particularly explains the effect of natural polymer drawing, which manifests itself in arising and development of a neck.[100] At annealing of an oriented glassy polymer above T_g, shrinkage of chains occurs under the action of entropic forces, and linking knots return to their equilibrium positions relative to each other.

Thus, in addition to orientation of molecules crazing is accompanied by the formation of a nanoporous structure, *i.e.*, development of an interface. Formation of a free surface in a glassy polymer is possible only if scission of a part of chains or disentanglement of knots takes place in the entanglement network.[101,102] Scission is favoured in polymers with high molecular mass and low density of entanglements (*e.g.*, PS), whereas disentanglement[102] is typical of low-molecular-mass polymers with high density of entanglements (*e.g.*, PS). In polymers like low-molecular-mass PC, chain scission dominates only at high rates of strain and relatively low temperatures, but entanglement also occurs around T_g and at low strain rates.[101,102] If chain scission dominates at crazing, full curing requires much longer annealing than in the case when the disentanglement mechanism prevails. This situation is illustrated by the data shown in Fig. 14.

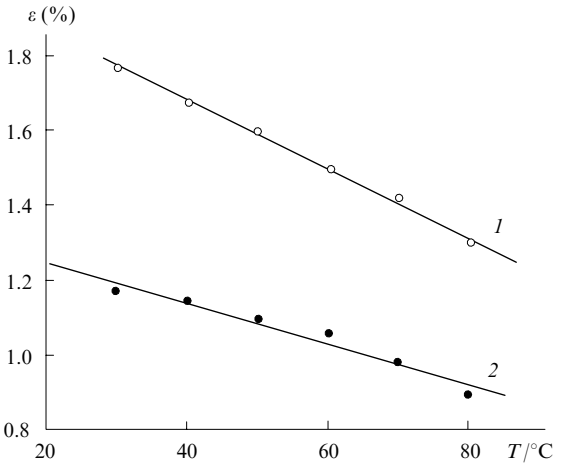

Figure 14. Temperature dependences of deformation initiating formation of crazes in PS.[99]
Before annealing (*1*), after annealing of crazed samples for 10 min at 130 °C (*2*).

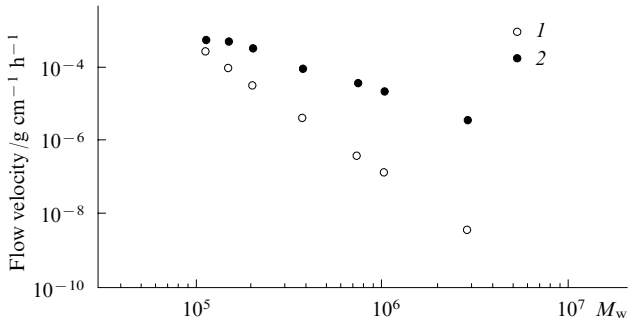

Figure 15. The flow velocity of PS melt in a macroscopic flow (*1*) and in a nanopore of 15 nm in diameter and 120 μm in length (*2*) *vs.* M_w of the polymer.[96]

Obviously, similar processes of the loss of a part of entanglements take place in solutions and melts of polymers when polymers penetrate into nanometre-sized pores since the processes of polymer assembling in nanometre-sized fibrillar aggregates in the craze structure and filling nanometre-sized cylindrical pores with polymer are analogous.

The loss of a part of entanglements during penetration of a polymer melt into nanometre-sized pores has a paradoxical effect on the molecular mobility of the polymer in the confined volume. Dependences of flow rates of a PS melt in macroscopic volume and a nanopore on the polymer molecular mass are presented in Fig. 15. As expected, in both cases the flow rate decreases with increasing the polymer molecular mass. However, the effect of the molecular mass on the polymer mobility is substantially lower in a confined volume (in nanopores) than in the bulky flow.[96] Viscosity in the bulk is usually proportional to the $(M_w)^{3.4}$ value if a molecular mass corresponding to formation of entanglements in the bulk is exceeded. At the same time, the exponent is equal to 1.5, but not to 3.4 in the case of nanopore (see Fig. 15). In other words, chain diffusion in nanopores is less dependent on the molecular mass. The entanglement network in solutions and (especially) melts influences the dynamics of polymer chains extremely strongly, therefore it influences the mass transfer processes: the greater the number of entanglements, obviously, the less intensive the chain dynamics and the slower mass transfer processes. Upon penetration of a polymer solution (melt) into narrow (comparable with the molecular coil size or even of a smaller diameter) pore, formation of the network is hindered, which affects the mass transfer processes.

III.2. The effect of spatial restrictions on diffusion mass transfer in polymers

The mass transfer in polymer solutions and melts which was considered above has its specifics related to the transport of macromolecules in through narrow pores. In this case,

external pressure favours penetration of a polymer into confined volumes even if the polymer coil size exceeds the pore diameter.

However, macromolecules are able to penetrate spontaneously into confined volumes even in the absence of an external force. Results of modelling and experimental observations [103] indicate that spatial restriction (the thickness of a layer in a film [94, 104] or the pore diameter in a porous material [105–107]) comparable to or smaller than the hydrodynamic radius do not hinder penetration of macromolecules in confined volumes.

It seems obvious that geometrical factor is a limiting factor for penetration of small particles into narrow pores if the particle diameter exceeds the diameter of pores. It is confirmed by the data on diffusion and flow of rigid protein molecules and polymers of low molecular mass through various porous media (compact silicon spheres,[108] porous quartz glasses,[109, 110] membranes with cylindrical pores produced with the use of accelerated heavy ions and subsequent etching [101–113]).

It may seem unusual that large flexible macromolecules deviate from this rule and penetrate more easily into small pores than spherical particles. Moreover, the effect of easier penetration of flexible molecules was observed when flow velocity and polymer concentration increased.[114–116]

Teraoka *et al.*,[117] who studied diffusion of PS with different molecular masses into porous glasses (with pore diameter of 27.5 nm) from solutions in 2-fluorotoluene, revealed that the apparent diffusion coefficient inside a pore rapidly increases with the solution concentration if it is higher than the crossover concentration. This increase is more pronounced for high-molecular-mass polystyrenes.

To study diffusion through cylindrical pores, PC filters with pores produced by bombardment of PC plates with accelerated heavy ions and subsequent etching were used,[107] the pore sizes in the filters were controlled by varying the etching time. It was found that diffusion is substantially hampered for dilute solutions where hydrodynamic radii of molecular coils are comparable with the pore radii. However, the diffusion of macromolecules into nanometre-sized pores is sharply facilitated at quite high concentrations. The diffusion kinetics becomes non-exponential and concentration dependent.

Adsorption of polyethylene oxide (PEO) with $M_w = 9 \times 10^3$, 78×10^3 and 1300×10^3 from aqueous solutions on glasses with pore diameters of 8 and 89 nm was studied.[118] Surprisingly, it was found that PEO with $M_w = 9 \times 10^3$ and 78×10^3 is instantly adsorbed on both types of porous glasses. The velocity of adsorption of PEO with $M_w = 1300 \times 10^3$ was slower (although quite comparable) than that of PEO with lower M_w. Unexpected behaviour was observed when sorbent with pore size of 8 nm was used. In this case, the adsorption velocity depended on the PEO solution concentration, decreasing with the decrease in the concentration (Fig. 16).

The presence of many plateaus observed at low polymer concentrations (see curve *3* in Fig. 16), in authors' opinion, reflects typical behaviour of individual chains, which have to unfold to penetrate into a pore. The plateau region in the plot corresponds to the situation when many individual chains are folded yet and have only slightly penetrated into pores, blocking the way to the pores for the other polymer molecules. This situation is eliminated at concentrations above the crossover point since entanglements between chains form continuous network in this case (see curve *1* in Fig. 16).

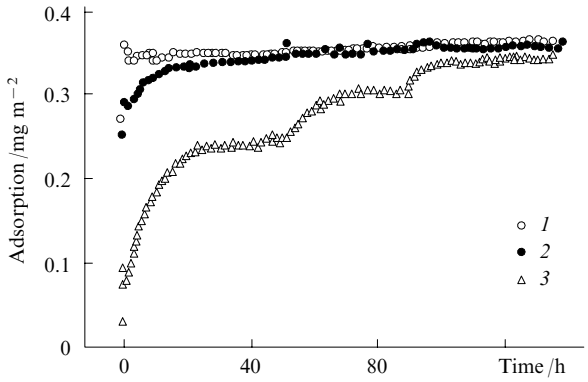

Figure 16. Kinetic plots of adsorption of PEO from its aqueous solutions on porous glass with pore diameters of 8 nm.[118] Initial concentrations of solution: 0.0157 (*1*); 0.0039 (*2*) and 0.0010 (*3*) g × cm^{-3}.

Finally, it is necessary to mention studies on introduction of macromolecules into nanoporous structure of developing crazes. Recall that crazing is one of fundamental types of inelastic deformation in glassy and crystalline polymers.[88] In the course of stretching in active liquids, polymers are deformed due to development of a nanoporous structure with pore sizes from a few to tens of nanometres, which are continuously filled with surrounding liquid. Attempts were made to insert a second polymeric component with rather high molecular mass (from 4×10^3 to 10^6) into the craze porous structure. Polyethylene oxides with these molecular masses are solid at room temperature, therefore their water–ethanol solutions were used to introduce them into PETP and high-density polyethylene (HDPE), which were deformed in these solutions.[119–121]

Surprisingly, it was found that polymers with these high molecular masses efficiently penetrate into nanoporous structure of crazed PETP and form nanocomposite based on two polymers. Electron micrographs of PETP crazed in a pure solvent and those of PETP strained in a solution of PEO with $M_w = 10^6$ are shown in Fig. 17. As can be seen, high-molecular-mass PEO penetrates into the nanoporous structure of the crazed polymer, efficiently filling it.

Deformation of PETP in a solution of PEO with molecular mass up to 10^6 makes it possible to prepare nanocomposites of two polymers with a significant content of the second component (Fig. 18). Recall that the penetration of PEO into the porous structure of PETP represents a case when the penetrating macromolecule coil sizes are considerably larger than the pore sizes of the polymer strained by the crazing mechanism. An effective diameter of the pores formed upon PETP deformation in adsorptionally active medium is equal to 5–10 nm according to the measurements with the use of the method of pressure-driven liquid permeability or small-angle X-ray scattering technique, whereas the hydrodynamic radius of macromolecule coils of PEO with molecular mass from 4×10^4 to 10^6 is 9.2–63 nm.[119] Moreover, the amount of PEO penetrating during crazing substantially exceeds the amount corresponding to the case when the porous structure is entirely filled with the polymer solution with the polymer concentration equal to its concentration in the bulk (see Fig. 18).

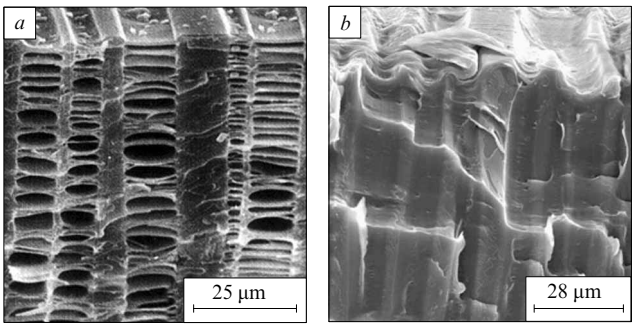

Figure 17. SEM images of PET samples strained by 100% in a pure adsorptionally active medium (*a*) and in 5% solution of PEO with molecular mass of 10^6 (*b*).[119]

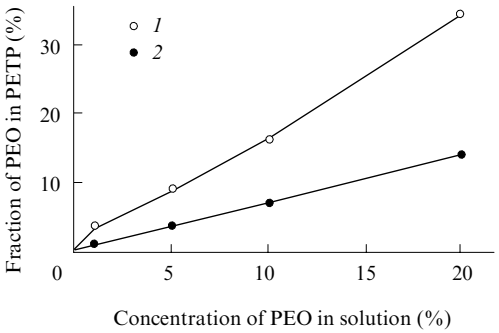

Figure 18. Amount of PEO with molecular mass of 4×10^4 which was included into PET during stretching of the latter in a water–ethanol solution of PEO *vs.* concentration of this solution (*1*) and calculated dependence of PEO amount which can be included into PET, assuming maximum filling the porous craze structure with PEO solution with the initial concentration (*2*).[122]

In other words, there is some mechanism ensuring an increase in the PEO concentration in the solution penetrating into the porous PETP structure, which was developed during crazing in the course of PETP deformation in a solution of another polymeric component (PEO).

It is important to notice that an analogous penetration of PEO macromolecules into the structure of a polymer deformed by crazing mechanism is also observed in the case of a pure diffusion when already crazed polymer is placed in a PEO solution of known concentration. PEO diffuses from its solution into the crazed polymer matrix, and the amount of adsorbed component appears to be close to that shown in Fig. 18.

Thus, diffusive transport of macromolecules into narrow (nanometre-sized) pores considerably differs from diffusive mass transfer of macromolecules during their adsorption from a solution on a planar surface.[123–125] The important specific feature of this transport is a sharp increase of the velocity of diffusion of macromolecules from solutions into pores, which is observed at high (above the crossover point) concentrations of polymers irrespective of their molecular masses. In other words, there are two modes of macromolecule diffusion into narrow pores: the fast mode, which is typical of solutions with high concentrations, and slow mode, which takes place in dilute solutions. Note that anomalously fast diffusion of a polymer from its concentrated solution is not hampered even if the size of unperturbed macromolecules is comparable with (or even exceeds) the diameter of pores where they penetrate. This raises the question about the mechanism of the observed phenomenon.

Diffusion in polymer solution is one of the oldest problems of physics of polymers.[126, 127] At least two mechanisms of macromolecule transport in solutions, which correspond to the two above discussed modes of macromolecule diffusion, are suggested. It is noteworthy in this connection that diffusion mass transfer is characterized by two diffusion coefficients: self-diffusion coefficient (D_s) and cooperative diffusion coefficient (D_c). The self-diffusion coefficient describes movement of macromolecules relative to surrounding molecules due to thermal motion, while the cooperative diffusion coefficient corresponds to movement of molecular ensemble in a density gradient.[128–132] For the cooperative diffusion of a polymer to take place, it is necessary that macromolecules are joined in a solution by a common entanglement network, which prevents their independent movement in the solution. It is generally accepted that sharp acceleration of diffusion in polymer solutions with concentrations higher than the crossover point is connected precisely with cooperative diffusion processes.

How do the macromolecules connected by the common entanglement network and having unperturbed sizes exceeding the pore sizes penetrate into these pores? The entanglements in the macromolecule network are described by an equivalent tube, which restricts mobility of separate chains.[126, 127] The movement of the chains in the tube is called reptation to emphasize the ability of flexible macromolecules to a molecular translational motion resembling the motion of snakes. Reptation of macromolecules in a solution makes it possible to understand and explain their penetration into narrow pores. The data obtained by Shenga and Wang[133] illustrate this. The authors studied static and nonequilibrium dynamic properties of a polymer chain by Monte Carlo simulations. The results are shown in Fig. 19. A polymer chain containing 50 units, being confined in cylindrical pores of various diameters, considerably changes its conformation. In fact, it was shown that the coil–stretched chain conformational transition takes place with increasing spatial restrictions. In other words, this transition can be initiated under the conditions of equilibrium diffusion (without phase flow) merely by a change in spatial restrictions of the polymer chain.

Dynamic behaviour of polymer macromolecules during their penetration in nanometre-sized pores was characterized theoretically[134] by calculation of separation coefficient, which is the ratio of particle concentrations inside and outside the pore, for flexible chains and rigid rods at infinite dilution. Later on, conformations of large flexible chains confined in small cylindrical pores were studied depending on the polymer concentration in a good solvent using a scaling approach.[135] It was demonstrated that flexible chain macromolecules are able to penetrate into confined volumes owing to reptation motion, which is, in essence, the movement caused by incessant changes in macromolecule conformations.

It is due to the conformational transitions that polymer chains can penetrate into very narrow confined volumes. It was shown[136] that chain molecules are also able to penetrate even into zeolite channels. A zeolite with channels of only 0.74 nm in diameter was used in this study, never-

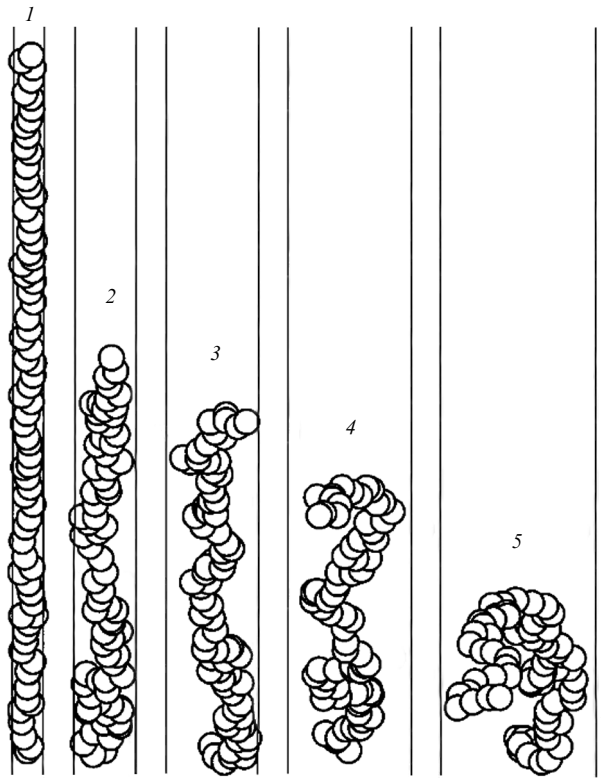

Figure 19. Conformation of a 50-unit polymeric chain which is confined within cylindrical pores with diameters of 2 (*1*), 4 (*2*), 6 (*3*), 8 (*4*) and 10 nm (*5*).[133]

theless (Fig. 20) not only ethylene glycol (curve *1*), but also its high-molecular-mass analogues with various molecular masses are sorbed into its structure. Furthermore, as can be seen from Fig. 20, high-molecular-mass homologues are sorbed much more efficiently than monomeric ethylene glycol. Even adsorption of polyethylene glycol with a polymerization degree of 900 in the region of relatively low equilibrium concentrations is many times greater than that of ethylene glycol. The authors suppose that penetration of polymer chains into so narrow pores is only possible due to reptation, whereas hydrophobic interactions of an adsorbed substance with pore walls can compensate entropy loss, which inevitably takes place when polymer coils penetrate into such narrow pores.

It is also necessary to touch briefly upon the driving forces which compel a polymer molecule to penetrate into narrow pores (see Fig. 19) in spite of substantial entropy losses, which accompany the conformational transitions noted above. Clearly, the penetration of polymer chains into narrow pores is caused by interactions of the polymer with the pore walls, *i.e.*, by adsorption of the polymer on the walls. On one hand, penetration of macromolecules into narrow pores should result in entropy loss due to reduction in the number of possible conformations of the chains located near walls,[133] but on the other hand, it should result in a gain in free energy due to non-zero value of segmental adsorption energy. This gain can compensate the entropy loss resulting from the compression of chains in pores. Hence, the chain concentration in pores should be higher if absorption takes place than if there is no absorption. This reasoning is schematically illustrated in Fig. 21.

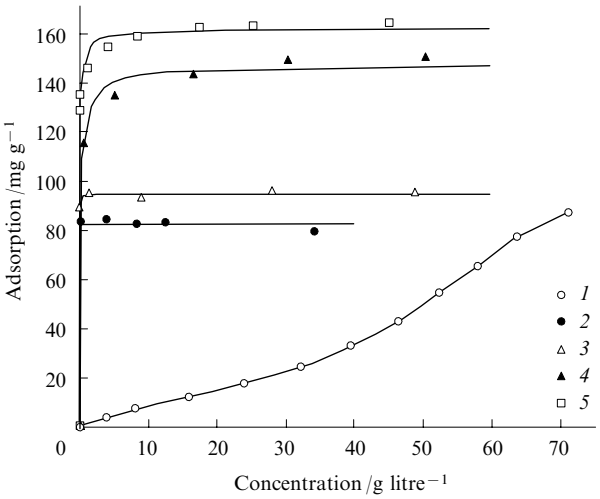

Figure 20. Isotherms for sorption of ethylene glycol (*1*) and PEO with polymerization degree of 900 (*2*), 200 (*3*), 6.8 (*4*) and 13.6 (*5*) by zeolite FAU.[136]

Both approaches (dynamic and static) predict that long flexible chans penetrate into small pores more easily if their concentration is higher. The experimental data qualitatively confirm this prediction,[115, 116] but quantitative comparison is difficult since it requires the use of identical polymer chains and perfect porous structures (cylindrical pores of a controlled radius).

In conclusion of this Section, it is necessary to note another possible contribution to the increase in free energy, which also favours penetration of macromolecules into narrow pores. It is operative in the case of crystallizable polymers (such polymers were used in the diffusion experiments in the majority of the referred above studies). Orientation of the polymer macromolecules during their penetration into narrow pores initiates orientational crys-

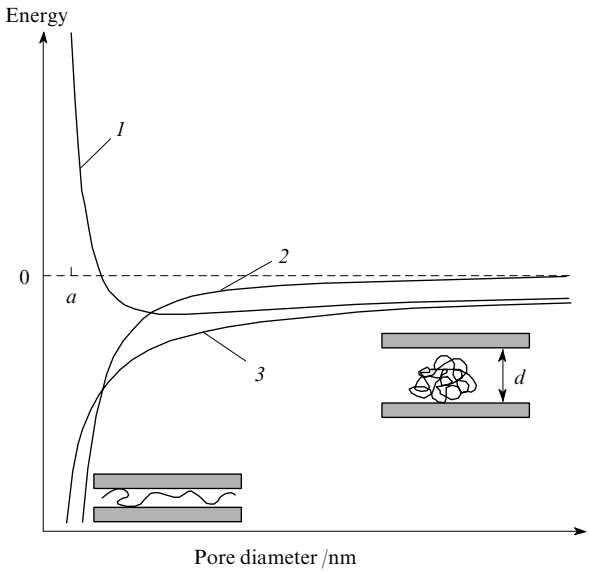

Figure 21. Free energy (*1*), entropy (*2*) and enthalpy of adsorption (*3*) *vs.* the diameter of a pore where macromolecule is adsorbed from a solution;[118]
(*a*) is the size of a monomeric unit.

tallization.[137] The heat of crystallization is significantly higher than the heat of adsorption, which, obviously, determines a higher gain in free energy.

IV. Effects of spatial restrictions on phase transitions in crystallizable polymers

The data considered above indicate that polymers ground to nanometre sizes acquire some properties untypical of bulk polymers. Naturally, spatial restrictions strongly influence phase transitions in crystallizable polymers. This influence should have the most strong impact on the crystallization processes since such a fundamental characteristic as the size of a phase nucleus has a decisive importance in the course of crystallization.[138] The typical size of a phase nucleus is from a few to tens of nanometres, therefore nanometre-sized spatial restrictions should undoubtedly have an impact on nucleation upon crystallization of polymers in the first place, and hence, should affect the polymer structure and properties.

IV.1. Effects of spatial restrictions on crystallization of polymers

Thin polymer films are usually used in studies of impact of nanometre volume restrictions on the structure and properties of polymers (see Section II).[59] In recent years, preparation of polymer nanotubes and nanorods has become widely used.[139–142] So called template-based method[143,144] consists in the synthesis of a polymer inside pores of a porous membrane and subsequent dissolution of the template membrane to isolate the polymer particles. A version of this approach consists in introduction of polymer melts or solutions into nanometre-sized pores of the template membrane by its wetting.[145,146] The driving force of penetration of a polymer in nanometre-sized pores can be external pressure.[147] This approach is also used to fill such ideal templates as anodic aluminium membranes with a polymer (see Fig. 10) and subsequently dissolve the aluminium matrix. Polymer nanotubes and nanorods were obtained in all referred studies.

SEM images of the prepared products are shown in Fig. 22. These images make it possible to analyze properties of the polymers in the nanoscale state. Properties of these nanoscale objects were the subject of numerous studies (*e.g.*, see Refs 8, 9, 13 and 148), and quite a few data have now been accumulated, which allow one to make some generalizations. For instance, it was demonstrated[93] that there is no molecular orientation in nanorods of syndiotactic PS in molten state in cylindrical pores of the aluminium matrix. If solid amorphous syndiotactic PS is heated above room temperature, it crystallizes in nanorods as in the bulk, forming crystals of the same degree of crystallinity and without preferable orientations. If syndiotactic PS crystallizes from melt in nanometre-sized pores, a structure with *c* axes normal to the nanorod axis is formed. Crystallinity in these nanorods is considerably lower than in the bulk, and the smaller the pores, the lower the crystallinity.

Aluminium templates were used[12] to explore effects of spatial restrictions on the crystallization of linear PE. The influence of a nanopore size on melting point (T_m) is demonstrated in Fig. 23 *a*, while the effect on degree of crystallinity of the polymer (α) is demonstrated in Fig. 23 *b*. It is clear that the volume of the PE phase has an impact on both T_m of the polymer and its degree of crystallinity.

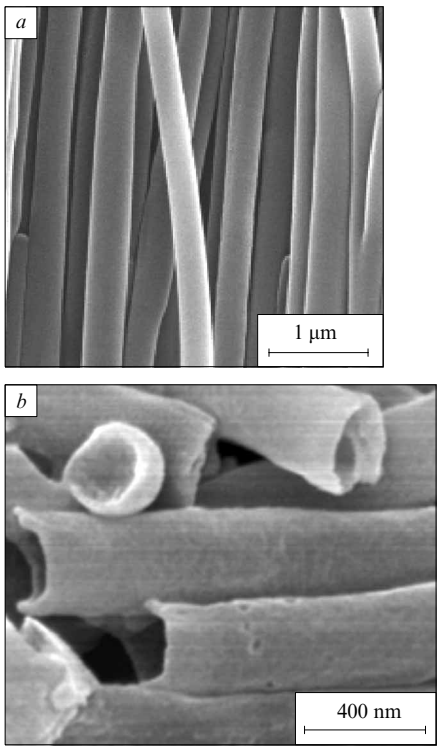

Figure 22. SEM images of nanorods of syndiotactic PS (*a*)[93] and nanotubes of polyvinylidene fluoride (PVF) (*b*).[8]
Nanorods and nanotubes were obtained by filling porous aluminium template with PS melt and PVF solution in dimethylformamide, respectively, and subsequent dissolution of the template.

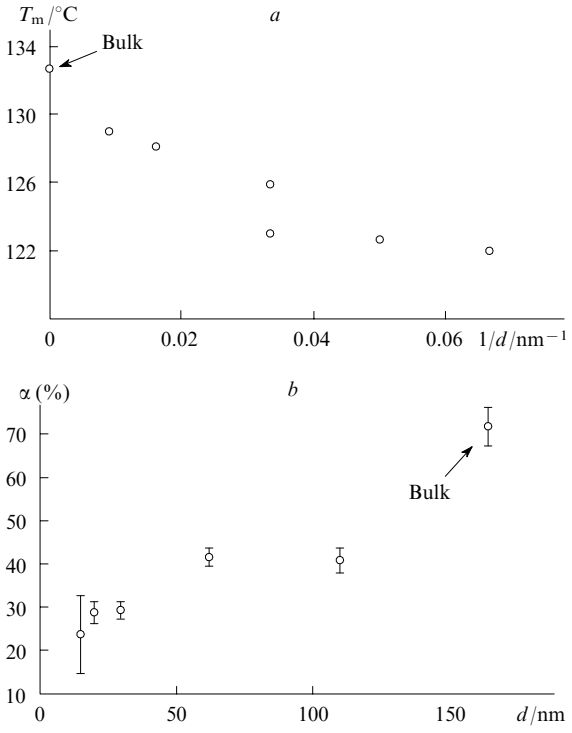

Figure 23. Temperature dependences of melting of linear PE (*a*) and its degree of crystallinity (*b*) on the pore diameter in an aluminium template, in which crystallization and melting were carried out.[12]

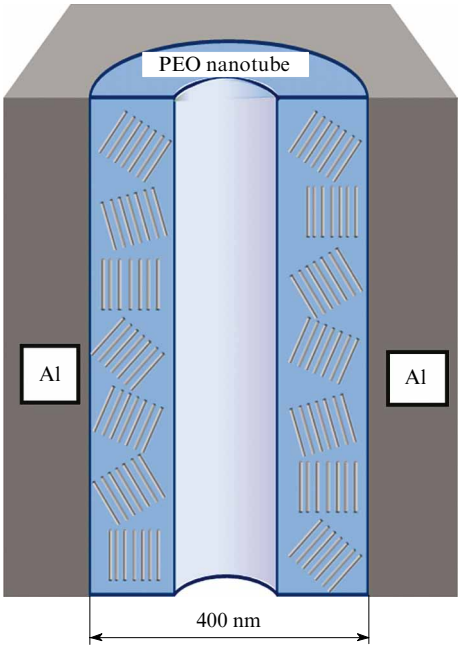

Figure 24. Diagram of PEO nanotube in a cylindrical aluminium template.[149]

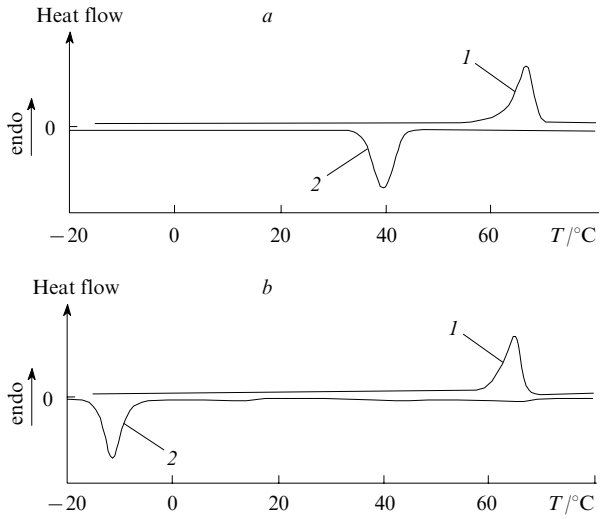

Figure 25. DSC thermograms of melting (*1*) and crystallization (*2*) of PEO in the bulk (*a*) and in a nanotube with wall thickness of ~100 nm (*b*).[149]

Thermal characteristics of PEO in the form of nanotubes with wall thickness of ~100 nm were investigated [149]. The tubes were prepared by impregnation of aluminium templates with cylindrical pores of 400 nm diameter with PEO solution or melt. The impregnation conditions were selected such that a cylindrical pore was partly filled, and a cylindrical void was formed at its centre (Fig. 24). The prepared samples were studied using differential scanning calorimetry (DSC). The DSC plots of the processes of crystallization and melting of bulky PEO and PEO in the form of nanotubes with the wall thickness of ~100 nm are shown in Fig. 25. As can be seen, the crystallization point in the latter case is lower by approximately 50 degrees.

Analogous dependences were also observed for processes of crystallization of nanotubes of polyvinylidene fluoride,[8] syndiotactic PS,[93, 150] PE,[12] some block copolymers [151] and other compounds.[152] The following generalizing conclusion was drawn:[12, 152] crystallinity of polymers decreases, supercooling degree (the difference $\Delta T = T_m - T_{cr}$) increases, and melting point decreases under nanometre volume restrictions.

Thus, volume restrictions also influence the mechanism of crystallization.[153] When crystallization mechanism is considered, the ratio of crystallization rate to supercooling degree is usually used. In large pores ($d > 50$ nm), crystallization occurs at small values of ΔT and strongly depends on T_{cr}. On the contrary, in smaller pores ($d < 50$ nm), crystallization occurs in wider range of ΔT, and its dependence on T_{cr} is less pronounced.[153] A strong temperature dependence of the crystallization rate in large pores can easily be interpreted in the framework of classical nucleation theory as kinetics of crystallization with homogenous nucleation.

One can conclude on the basis of analysis of published data that the nucleation process prevails over the nucleus growth process during polymer crystallization in a confined volume. This has an effect on the structure and properties of the produced product. Homogeneous nucleation occurs in a bulk polymer and is related to density fluctuations. As a result, no preferable direction of crystallite growth is observed. On the contrary, the wall of a narrow pore plays a role of a substrate for heterogeneous nucleation. This important specifics of polymer crystallization in narrow pores is demonstrated in Fig. 26. As can be seen, crystallization of a polymer is accompanied by crystallite orientation relative to the pore axis. It is noteworthy that during heterogeneous nucleation occurring in narrow pores, supercooling is much lower than during homogeneous nucleation. The high supercooling observed experimentally during

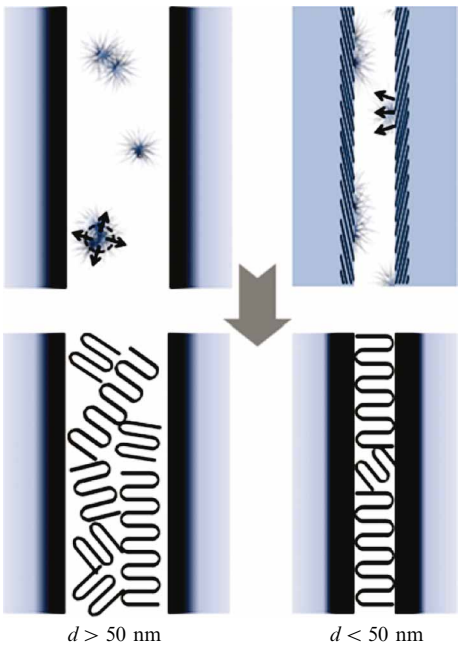

Figure 26. Diagram of nucleation (above) and crystallization (below) of a polymer in wide (>50 nm) and narrow (<50 nm) pores.[154]

crystallization of a polymer in narrow pores was attributed to diminution in crystallite sizes and increasing interfacial areas.[149]

There is also a possibility of homogeneous nucleation in confined nanoscale phases of crystallizing polymer such as nanoscale droplets.[155–158] Crystallization occurs in practically monodisperse droplets of ~100 nm size. In this case, the transition from heterogeneous to homogeneous nucleation is determined by existing geometrical restrictions. First, under these conditions, a crystallizing polymer is not in contact with any solid surface, therefore the posiibility of heterogeneous nucleation is practically eliminated. Second, a small number of randomly formed nuclei, which are always present in a real bulk polymer and responsible for heterogeneous nucleation, is distributed over a large number of droplets, therefore the nuclei are present not in all droplets and, thus, they cannot efficiently influence the crystallization process.[159,160] In the absence of heterogeneous nuclei, homogeneous nucleation occurs in a droplet, therefore strong supercooling is required under these conditions. This situation is illustrated by Fig. 27. As can be seen, dispersion of a polymer in a microemulsion results in a sharp increase in supercooling, and, probably, homogeneous mechanism of nucleation really operates in this case.[161]

There is another way to ascertain the regularities of polymer crystallization under spatial restrictions. Spatial restriction of polymer layers of virtually any size can be accomplished by so-called forced assembly of multilayer polymeric systems. The process of layer multiplication is based on the use of viscoelastic properties of polymer melts during coextrusion of two polymers, which results in the consecutive increase in the number of layers of incompatible polymers in a formed film. Multilayer systems on the basis of incompatible polymer pairs are convenient objects for experimental studies of the structure of polymer blends.[162–167] Improvement of the process of multilayer coextrusion made it possible to reduce the layer thickness by two orders of magnitude, from microscale to nanoscale.[168]

Clearly, if a crystallizable polymer is taken as one of the components, the effect of spatial restrictions on its crystallization can be studied. Indeed, multilayer films consisting of thousands of alternating layers of amorphous PS and crystallizable PEO were obtained using coextrusion.[169] It was found that with decreasing the PEO layer thickness, the morphology initially changes from three-dimensional spherulites to two-dimensional discoids. Starting from a layer thickness of 25 nm, PEO crystallizes in the form of separate lamellas resembling an ensemble of polymer single crystals. It was unexpectedly found that oxygen permeability sharply (by 2 orders of magnitude) decreases with the decrease in the thickness of PEO layers. This effect is assumed to be related to the morphology of the crystalline phase, where tortuosity of the diffusion way for a low-molecular-mass component significantly increases. Later on, it was demonstrated that crystallization rate sharply decreases with decreasing the PEO layer thickness.[170]

Deceleration of polymer crystallization in thin (nanometre-sized) layers is a general phenomenon. As noted above, under volume restrictions, the degree of crystallinity of a polymer (see Fig. 23) and the rate of crystallization considerably decrease.[171–174] For example, the rate of crystallization of PEO in thin layers (13 nm–2 μm) can decrease 40-fold as compared to the rate of bulk crystallization starting from a thickness of 150 nm.[175] Simultaneously, the crystal morphology changes.

Crystallizaytion of PEO adsorbed as a monolayer on a silicon surface was studied [176]. When the system was cooled, crystallization of the adsorbed layer started. The diagram of structural transformations accompanying the crystallization is shown in Fig. 28. Crystallization is initiated on some heterogeneous nucleus and proceeds by vertical attachment of macromolecules with formation of a lamellar structure. Clearly, the attachment of molecules to a crystal leads to energy release. This energy release is larger if molecules are attached vertically because in this case each of them has more neighbouring molecules. The critical stage of this process is the transport of molecules to the site of crystallization, which is limited by diffusion.[177] The change in the structure from chaotic distribution of macromolecules over the adsorbed layer to their vertical orientation results in depletion of the area behind the crystallization front, owing to which a free (or empty) area appears on the surface since the area occupied by adsorbed molecules is larger than the area occupied by vertically crystallized molecules. To be attached to the crystal, a molecule should diffuse through this empty area. Naturally, this diffusion limits and strongly decelerates the entire rate of crystallization.

Crystallizable polymer adsorbed on a solid substrate has a disordered structure (see Fig. 28). Crystallization starts only under annealing of layers when molecules become sufficiently mobile. This crystallization is considerably slower than the crystallization in the polymer bulk as a rule. In this connection, it is necessary to mention studies of processes of crystallization in confined volumes which are

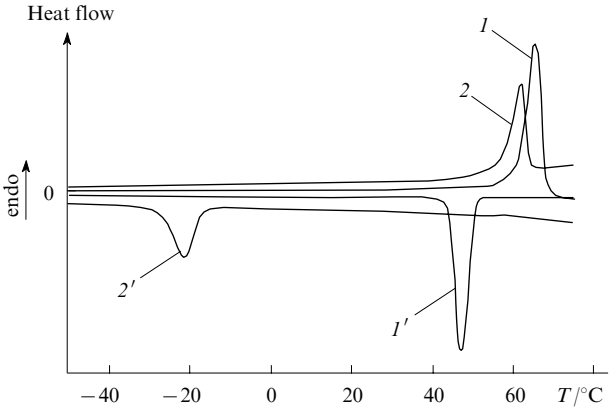

Figure 27. DSC thermograms for PEO (with molecular mass of 40×10^3) in the bulk (*1*, *1′*) and in the form of microemulsion (*2*, *2′*).[161]
Heating (*1*, *2*); cooling (*1′*, *2′*).

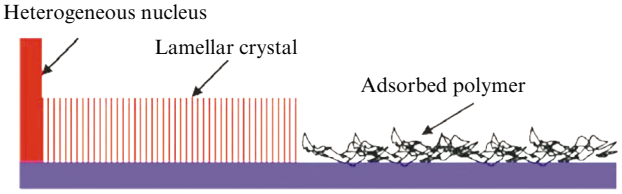

Figure 28. Diagram of structural transformations accompanying growth of a lamellar crystal from a thin layer of adsorbed polymer.[176]

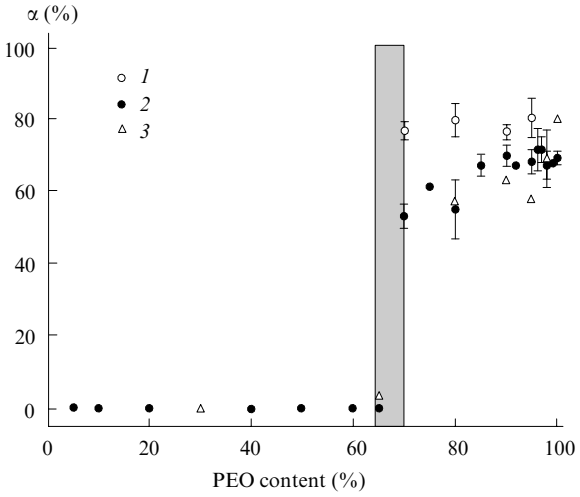

Figure 29. Degree of PEO crystallinity *vs.* its content in montmorillonite according to the data of X-ray diffraction (*1*), DSC (*2*) and Raman scattering (*3*).[184]

realized when crystallizable polymer is intercalated in laminated silicates (montmorillonites).[178–184] Pores in these silicates can be filled (intercalated) with a polymer. The introduced polymer is localized in layers of 0.8 nm thickness between silicate layers. Using melts or solutions of a polymer of different concentration, one can fill these pores to varying degrees.

Chrissopoulou *et al.*[184] intercalated PEO in different amounts into montmorillonite and then studied its crystallization in nanopores. It was found that at initial stages of filling nanopores in the laminated silicate, PEO does not crystallize (Fig. 29). However, when the amount of PEO becomes substantial, intensive crystallization starts with formation of the solid polymer with rather high degree of crystallinity, which increases with increasing PEO content. It can be assumed that, similarly to the case of crystallization of PEO in a monolayer, which was considered above, adsorbed layers of the polymer introduced into nanopores are unable to crystallize, and only imparting mobility to the polymer by annealing (see Fig. 28) or formation of sufficiently extended phase (see Fig. 29) results in crystallization of the polymer in such a confined volume.

IV.2. The effect of molecular orientation on the specifics of polymer crystallization

Recall that a solid crystalline phase is usually formed from melts or solutions of polymers. Therefore, it is necessary to dwell shortly on principal ideas about structural transformations, which occur in polymers during their flow.

During a flow of a polymer solution or melt under shear and stretching deformations, unfolding and mutual orientation of the macromolecules take place. At the same time, conformational transition and relative orientation of macromolecules influence their interactions between each other and with solvent molecules, and this can cardinally change the polymer–solvent phase diagram.[185] A thermodynamically stable transparent solution of a polymer can undergo phase separation only under action of an external mechanical field if temperature and composition (concentration) of the solution are constant.

In this review, we restrict ourselves to only a brief mention of phase separation with the release of the crystalline phase of a polymer from a solution under the influence of mechanical stress. Crystallization of polymers from solutions and melts owing to mechanical impact was observed in many studies. This phenomenon was considered in detail in a monograph [186] and several reviews.[187–189]

Systematic study of PE crystallization from flowing solutions was carried out.[190–193] It was found that in the flow, the temperature of crystallization of a polymer increases by 15–20 degrees, while the crystallization rate increases by several orders of magnitude. For the first time, the effect of shear stress on the boundary curve location at crystalline phase separation was studied in detail by Malkin and Kulichikhin.[194] These authors showed that the boundary curve is shifted to higher temperatures in a mechanical field. This shift depends on the shear rate and is caused by the decrease of the system entropy due to unfolding of macromolecules and their orientation in a flow.

One can briefly summarize the main propositions concerning the influence of flow on the characteristics of crystallization of polymers from their solutions and melts. As noted above, this influence is mainly connected with stretching of chains and their mutual orientation in a flow.[195, 196]

This orientation is a factor which induces orientation crystallization. The *in situ* studies using small- and wide-angle X-ray scattering afford direct proofs of formation of crystals in solutions and melts under the action of mechanical influence only.[197–200] Small-angle X-ray scattering was applied to study crystallization of PEO with molecular mass of $\sim 10^3$ in its melts at shear rates varied from 0.1 to 100 s^{-1} directly in a rheometer cell.[137] It was shown that orientation crystallization of PEO occurred at all shear rates. The shear rate considerably affects the structure of formed crystals: in the region of high rates, the large lattice spacing of the crystals initially increases, reaches a constant value and then decreases; at low rates, the large lattice spacing merely decreases. This difference was connected by the authors with the specifics of nucleation in flowing polymer melt.

Thus, mutual orientation of macromolecules in the liquid phase can result in their crystallization long before reaching the equilibrium T_{cr} value. It is also necessary to note that spatial restrictions in solutions and melts of polymers influence the processes of macromolecule orientation as well.

Orientation of PE crystallites in nanopores after impregnation of an aluminium template with the polymer melt was studied with the use of X-ray diffraction.[95] It was found that under these conditions, PE crystallizes with formation of pronounced textures, and orientation of crystallites depends on pore diameters (Fig. 30).

It is important to note that asymmetric crystallites are oriented along pore axes, whereas the *c* axes of macromolecules are normal to their principal axes. It was also reported that orientation of chains of PVF,[8] syndiotactic PS [93] and PE [201] in aluminium templates of different sizes is normal to the pore walls.

At the same time, if polymer is synthesized directly in nanopores, normal chain orientation relative to the pore walls can be broken. In particular, it was shown that conductive polymers prepared in nanotubes can have both parallel and normal orientation relative to the pore axis.[202, 203]

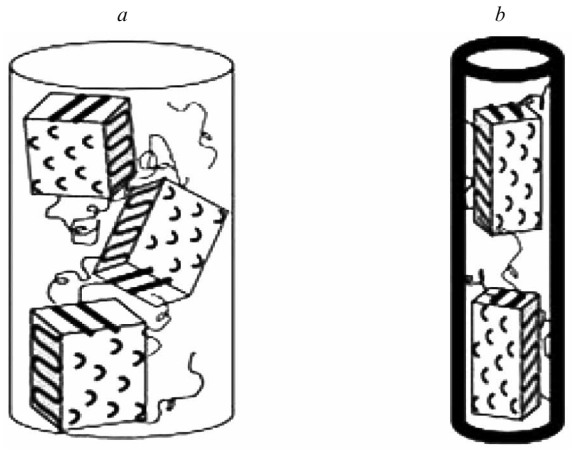

Figure 30. Diagram of oriented packing of crystallites in wide (> 50 nm) (*a*) and narrow (< 50 nm) (*b*) cylindrical pores.[95]

IV.3. The effect of crystallite size on the melting point and heat of melting of polymers

A noted above, if polymer crystallizes in nanopores, the nucleation stage prevails over the nucleus growth stage, which naturally results in formation of a product containing very small crystallites. The decrease in the crystallite sizes leads to an increase in the interfacial surface and, hence, to a depression in the melting point.

The Gibbs–Thomson equation is widely used to describe the T_m dependence on the crystallite size and interfacial surface energy [187–189]

$$\Delta T_m = T_m^\circ - T_m = \frac{4\sigma T_m^\circ}{d\Delta H_m \rho_{cr}} \quad (3)$$

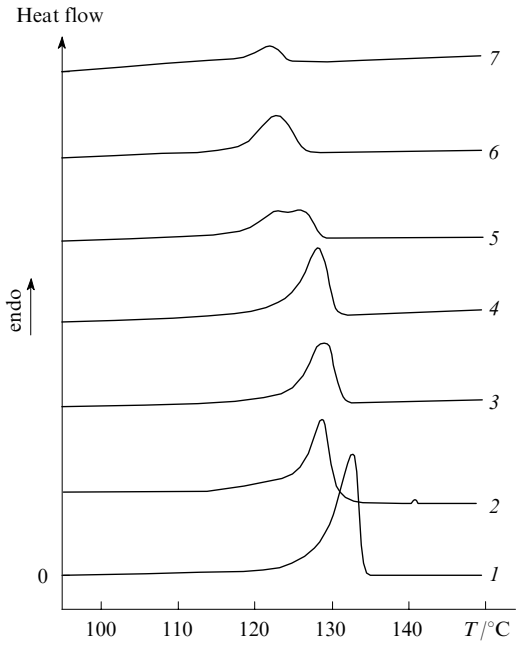

Figure 31. DSC thermograms of bulk PE (*1*) and PE crystallized in nanoporous aluminium templates with pore diameters of 220 (*2*), 110 (*3*), 62 (*4*), 30 (*5*), 20 (*6*) and 15 nm (*7*).[12]

where T_m° is the equilibrium melting point of an infinite crystal, σ is the interfacial surface energy, ρ_{cr} is the crystal density, ΔH_m is the specific melting heat, d is the crystallite size (in the case of melting in a confined volume, d is the size of nanopores where polymer was crystallized). As follows from the equation, the temperature decrease is inversely proportional to the nanopore diameter.

The DSC thermograms for melting of PE in narrow cylindrical pores of various diameters are shown in Fig. 31. As can be seen, the melting point significantly decreases with decreasing the pore diameter.[12] Expanding melting point range is attributed to the transition from homogeneous nucleation at bulk crystallization to heterogeneous nucleation in narrow pores, which results in the change in morphology of the formed product.

It is necessary to note in conclusion that melting heat also depends on the applied spatial restrictions. Particularly, this dependence manifests itself in the influence of the diameter of pores where polymer crystallizes on the crystallinity degree of the product (see Fig. 23 *b*).

V. Crazed polymer as a matrix creating spatial restrictions

As it was noted above, crazing of a polymer is, in essence, a method for its dispersion into extremely small (nanometre-sized) aggregates of oriented macromolecules (see Fig. 12). The development of this unique structure is only possible if an active liquid is supplied into the region of the local transition of a polymer into the oriented state timely and in sufficient amounts.

Since the pore sizes in a crazed polymer do not exceed several nanometres, crazing is an efficient approach to dispersion of not only polymers, but also other compounds dissolved in an adsorptionally active medium. Thus, crazing opens a possibility of preparation and study of almost any compounds in the superfine nanometre-sized state. In contrast to the above considered methods for preparation of solids with the purpose of elucidation of the effects of nanometre volume restrictions on their properties (aluminium templates, filters with pores produced by bombardment with accelerated heavy ions, nanoporous glasses, *etc.*), crazing is an amazingly simple and accessible method. Indeed, to prepare a compound dispersed down to nanometre-sized aggregates, it is sufficient to stretch a film of almost any synthetic polymer in a melt or solution of this compound. It is important that this approach makes it possible to carry out a comparative analysis of effects of spatial restrictions on crystallization of polymers and low-molecular-mass compounds.

The first example of such studies was the investigation of effects of nanometre volume restrictions on the structure and properties of low-melting n-octadecane (OD) (T_m = 28 °C).[204] A PETP film was stretched in liquid OD at 50 °C and cooled in clamps of a stretching device. Due to this procedure, OD, being an efficient adsorptionally active medium, fills the craze porous structure and then crystallizes. By this simple method, one can obtain nanocomposites: a crystalline compound is introduced in a polymer matrix in a form of finest aggregates, which, obviously, are not larger than the diameters of pores in the craze structure (from a few to tens of nanometres). The obtained product makes it possible to explore the characteristics of the introduced low-molecular-mass compound under nanometre-scale spatial restrictions.

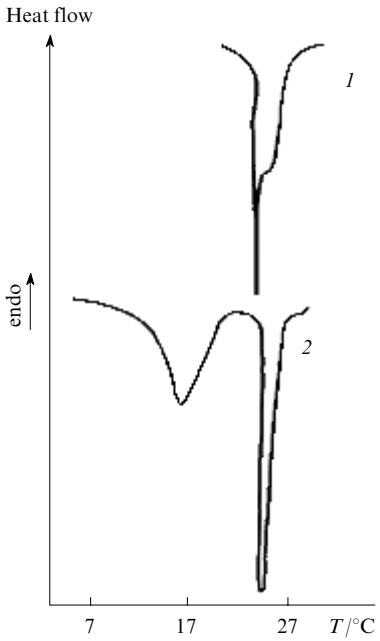

Figure 32. DSC thermograms of crystallization of OD (*1*) and OD in crazes in PET (*2*).[204]
The stretching degree of PET in OD is 50%.

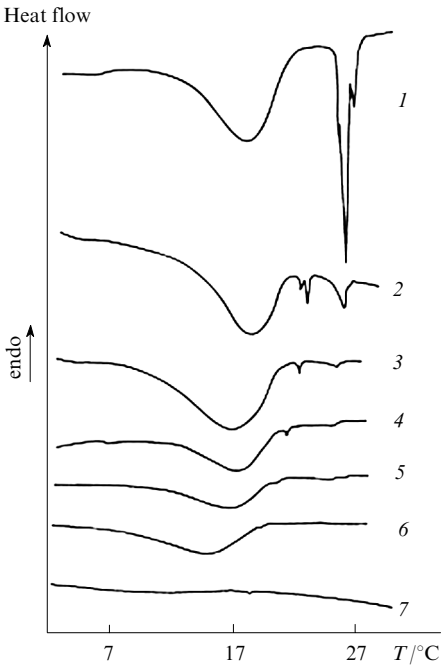

Figure 33. DSC thermograms of crystallization of PET samples which contain OD and were obtained by washing in n-heptane for 0 (*1*), 5 (*2*), 10 (*3*), 15 (*4*), 20 (*5*), 30 (*6*) and 60 min (*7*).[206]

Typical calorimetric curves for crystallization of a saturated hydrocarbon (OD) in the bulk and after inclusion into the PETP porous structure are presented in Fig. 32.[204] As can be seen (see curve *1*), the hydrocarbon crystallizes in the bulk at 24 °C (the asymmetric peak, whose shape is, possibly, caused by a transition from orthorhombic to hexagonal packing, which is known to occur in the melting region of saturated hydrocarbons).[205] The spatial restrictions influence the thermal characteristics of OD in the polymer matrix: OD crystallization seems to proceed in two steps (see curve *2*). At first, a transition coinciding by temperature with the transition in bulk OD occurs. It is followed by quite a wide exothermic peak at the temperature lower by 6 – 8 degrees than the crystallization temperature of bulk OD. The major contribution ($\sim$ 80%) to the overall heat of crystallization is made at the second stage corresponding to the wide low-temperature peak.

The causes of this difference can mainly be elucidated by a study of the process of removal of OD from the porous structure of PETP. It was found that the use of some solvents makes it possible to remove a major part of introduced OD, while a substantial part of OD still remains in the polymer matrix. Calorimetric curves of crystallization for PETP samples which were subjected to washing with n-hexane are shown in Fig. 33. First, the fraction of n-octadecane whose crystallization temperature coincides with the crystallization temperature of bulk OD is removed during washing (see curves *1*, *2*). During further washing, the other fraction of OD which is responsible for low-temperature wide peak is also removed gradually (see curves *2* – *7*). Although prolonged washing results in complete disappearance of temperature transitions in the system PETP – n-octadecane and disappearance of the corresponding reflections in X-ray diffraction patterns, a substantial portion of the hydrocarbon (up to 30 mass %) still remains in the craze nanoporous structure.

Obviously, the peak corresponding to high-temperature crystallization is due to some small amount of OD localized on the sample surface in macroscopic pits or in large pores. Naturally, this part of OD is indistinguishable by its thermal characteristics from bulk n-octadecane. Probably, the wide low-temperature peak of crystallization corresponds to the fraction of OD located in the porous structure of the polymer crazes. The decrease in the crystallization temperature is caused by the dependence of the phase transition temperature on the size of the formed crystal nucleus. According to the formal theory of nucleation, the lower the nucleus size or lenght of the area of a new phase, the lower the crystallization temperature.[207] From the magnitude of supercooling, one can estimate the characteristic size of the crystal nucleus formed during crystallization of bulk OD. The size calculated from the DSC data was $\sim$ 16.5 nm. This value considerably exceeds the size of the most part of the pores in the structure of PETP strained in an adsorptionally active medium. The size of the crystallizing phase restricted by pore walls and the length of a pore are smaller than the size of a nucleus in bulk OD, therefore the crystallization temperature of the dispersed compound significantly decreases.

The pore size distribution in the polymer is rather wide since the low-temperature peak of crystallization is extended along the temperature scale. It is possible to estimate the pore size distribution in the polymer strained in this adsorptionally active medium from the peak shape. The procedure of the estimation is given by Volynskii *et al.*[204] The obtained results are shown in Fig. 34, they represent the size distributions of pores for samples of PETP stretched in OD by 50% and 400%. Stronger stretching of the polymer results in a considerable decrease in the pore effective radius, which was determined from the decrease in the crystallization temperature. This correlation agrees with known data of evolution of the polymer porous

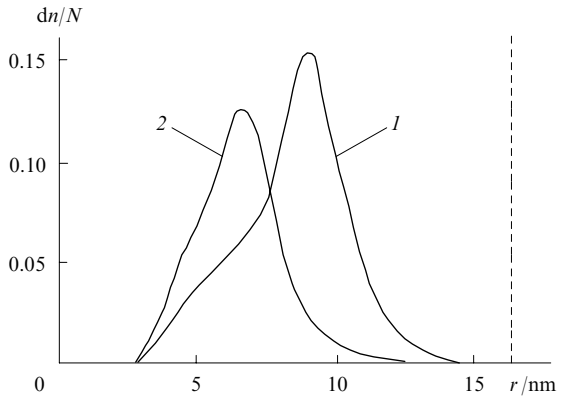

Figure 34. Plots of size distribution of pores in the structure of PET samples strained in OD by 50 (*1*) and 400 (*2*)%.[204]
Dashed line intercepts the abscissa axis at the point corresponding to the critical size of the nucleus of crystallization of free OD.
dn/N is the probability of the distribution.

structure during its straining in adsorptionally active medium, which were obtained using other experimental methods.[206]

However, the distribution curves cannot completely describe the polymer porous structure. As shown above, a substantial amount of OD remains in samples after washing. It was found [204] that the fraction of n-octadecane which cannot be removed from the craze structure by washing increases with the increase in the polymer stretching degree and amounts to $\sim 30\%$. In a crazed polymer strained in an adsorptionally active medium up to high stretching degrees, there are closed internal microvoids inaccessible to a solvent, from which the introduced low-molecular-mass compound cannot be retrieved by extraction. These voids are formed due to collapse of the craze structure at large polymer stretching. At the same time, these closed voids are so small that OD present there cannot form an extended crystalline phase. Therefore no phase transition is detected in DSC thermograms, and no reflection typical of the OD crystalline structure is present in X-ray diffraction pattern. This effect opens an interesting possibility to estimate the size of a molecular aggregate to which the thermodynamic conception of phase is not applicable. In the case of n-octadecane, this size is equal to ~ 2.5 nm (see Fig. 34).

It was demonstrated in subsequent studies that specifics of phase transitions for low-molecular-mass compounds in crazed polymer matrices (widening phase transitions and their shift to low temperatures), which were considered above, are general in nature. The same features are observed for different low-molecular-mass compounds (hydrocarbons, fatty acids and alcohols) and for almost all crazed polymers (PETP, HDPE, polypropylene, polyamide-6, polytetrafluoroethylene, PMMA, polyvinyl chloride).[206] Obviously, the generality of these phenomena is determined by the specifics of the craze fibrillar-porous structure.

Crystallization of polymers in confined nanometric volumes which was discussed above has much in common with the same process for low-molecular-mass compounds. The following features can be considered as common: phase transition widening, its shift to low temperatures and inability of the compound introduced into crazes to crystallize if the pore size is too small. As shown above, crystallization of polymers in nanometre volumes leads to a sharp decrease in the degree of crystallinity (see Fig. 23). Possibly, the major reason for this effect consists in inability of a polymer located in too small pores to crystallize.

The considered specific features of thermal characteristics of low-molecular-mass compounds inserted into the craze structure are connected with the conditions of their crystallization in narrow (1 – 30 nm) pores. The small size of pores is not the only factor; the approximate parallel arrangement of fibrils in the craze structure is another important factor (see Fig. 12). In this case, narrow asymmetric pores separating single fibrils are also mutually oriented relative to the axis of polymer stretching. Strongly pronounced asymmetry of the craze structure should have an effect on the crystallization of low-molecular-mass compounds in their volume.

This effect was revealed and investigated in an X-ray diffraction study of a number of systems crazed polymer – low-molecular-mass filler.[206, 208 – 210] It was found that irrespective of the used polymer and the nature of a crystallizing compound, low-molecular-mass compounds always crystallize forming highly ordered textures. This phenomenon is illustrated in Fig. 35 taking crazed PETP and PC containing various low-molecular-mass compounds as examples.

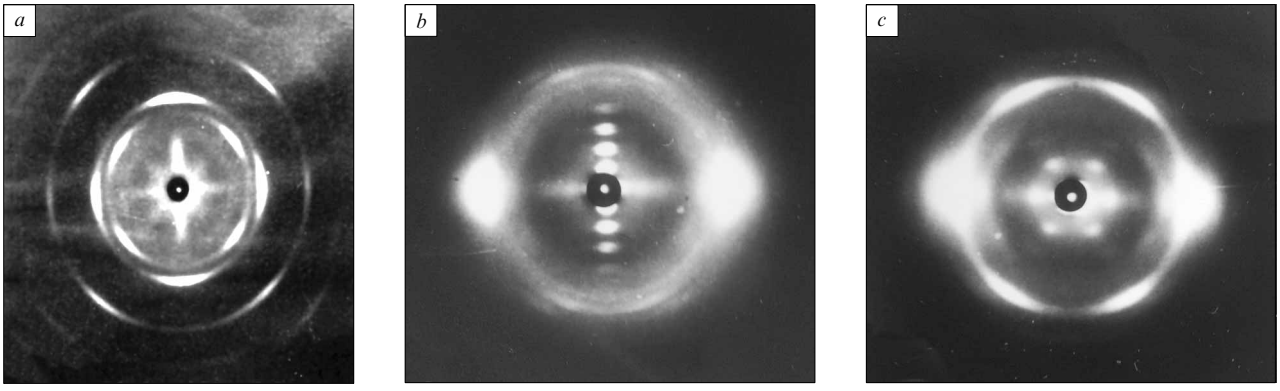

Figure 35. X-Ray diffraction pattern of crazed PET samples containing KI (*a*) and OD (*b*) and a crazed PC sample containing pentadecanoic acid (*c*).[206]
The axis of stretching of the polymers in an adsorptionally active medium is vertical.

As can be seen, the low-molecular-mass compounds crystallize with formation of highly ordered textures, and their X-ray diffraction patterns resemble X-ray patterns of single crystals. This phenomenon is of a general nature and is observed if both crazed crystallizable (PETP, PC) and amorphous (atactic PMMA) polymers are used as a matrix. All the specific features remain unchanged irrespective of the type of the crystal (ionic or molecular) formed by the introduced compound. It is important to note that crystallization of low-molecular-mass compounds like that of polymers (see Fig. 30) is accompanied by orientation of crystallites irrespective of the nature of these compounds.

Nevertheless, apart from the listed similarities in the crystallization of polymers and low-molecular-mass compounds under volume restrictions, there are also differences due to chain structure of polymers. These differences are observed when crystallization of polymers and low-molecular-mass compounds of similar chemical nature are studied. Consider the morphology of OD crystallized in a craze structure. Several series of meridional reflections are clearly seen in this case (see Fig. 35 *b*). An estimation of the large lattice spacing gives an exact value of the hydrocarbon chain length for OD. It means that OD crystallizes in regular layers, where hydrocarbon chains are oriented along the axis of an asymmetric pore in the craze structure of a matrix polymer. At the same time, a linear hydrocarbon crystallizes with formation of folded crystals, in which the *c* axes of macromolecules are orthogonal to the main pore axis (see Fig. 30). As can be seen, spatial restrictions influencing the crystallization of a compound in nanometre volumes are determined not only by interactions of this compound with the pore walls, but also by the ratio of the pore diameter and the size (chain length) of molecules of this compounds.

Concluding this section, it is necessary to make assumptions concerning the nature of the phenomenon of orientation of low-molecular-mass compounds in the structure of crazes which was revealed and described by Volynskii and co-workers.[206, 209, 210] Orientation effect of a crazed polymer matrix on crystallization of introduced low-molecular-mass compounds cannot be called epitaxy. Epitaxy is formation of uniformly (relative to each other) oriented cryatals of one compound on a face of a crystal of another compound.[211] As it was shown,[206] low-molecular-mass component crystallizes with formation of highly ordered textures no matter whether the crazed polymer matrix is crystalline or amorphous. Apparently, in the case under consideration, the major orientation factor is a strictly ordered arrangement of asymmetric pores in the craze structure (see Fig. 12).

Nevertheless, crystallites, but not individual molecules of a low-molecular-mass component are oriented in the craze structure. In particular, it is testified by the dependence of IR dichroism (a band at 2925 cm^{-1}) and heat of melting of tridecanoic acid (TDA) in a crazed PETP matrix on the content of the low-molecular-mass component (Fig. 36). The content of TDA in the polymer matrix can be controlled carrying out crazing of the polymer in its solutions of different concentration. As follows from Fig. 36 (see curve *1*), the heat of melting of TDA decreases in the whole range of its concentrations. Apparently, it is due to the decrease in the size of formed crystallites with decreasing content of TDA in the crazed matrix. The decrease in the size is accompanied by the increase in the specific surface area and, hence, by the decrease in the heat of melting since the crystallite surface layer possessing no

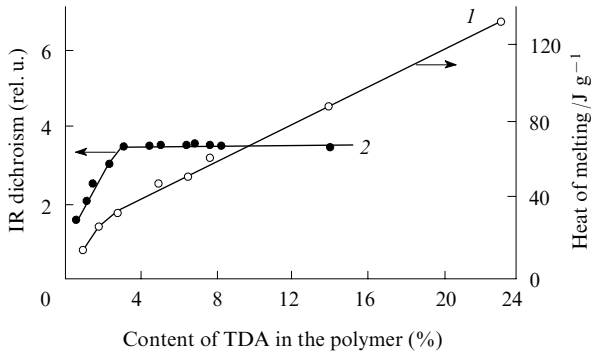

Figure 36. Heats of melting (*1*) and IR dichroic ratios of an absorption bans at 2925 cm^{-1} (*2*) of TDA introduced into a crazed PETP matrix *vs.* the TDA content in the polymer.[208]

three-dimensional crystal lattice makes no energy contribution to the melting process.

At the same time, the dichroic ratio in the IR region, which characterizes the degree of orientation of a low-molecular-mass component in the polymer matrix, changes in a different way (see curve *2* in Fig. 36). Orientation of TDA remains the same until its content in the polymer matrix is no less than 3%. When this concentration threshold is reached, IR dichroism sharply decreases (apparently, when the TDA content is above 3%, this compound mainly exists in the crystalline state in the polymer matrix). Further decrease in the TDA concentration results in its molecular dispersion in the volume of a craze, therefore the introduced component becomes in the adsorbed, but not crystalline state. It is clearly seen that the fraction of the crystalline phase starts to decrease sharply in this concentration region. This result indicates that there is orientation of crystallites, but not individual molecules in the craze structure. This agrees with the data of the study considered above [176] (see Fig. 28) where it was shown that a polymer layer adsorbed on a solid surface has disordered structure. Naturally, crystallization of this layer imparts molecular ordering to it.

VI. Conclusion

The above analysis of literature data indicates that the dispersion of polymers to nanometre-sized aggregates critically changes their properties. These changes concern the polymer fundamental characteristics such as glass transition temperature and phase transitions in crystallizable polymers. Spatial restrictions considerably influence the mass transfer in solutions during their flow or diffusion. First of all, these effects are caused by conformational rearrangements of polymer chains under nanometre volume restrictions. The changes in conformations of macromolecules and existence of entanglement network are responsible for sharp depression in glass transition temperature in thin films and anomalies in the processes of sorption, diffusion and flowing of polymer solutions and melts. Spatial restrictions affect both parameters of phase transitions in crystallizable polymers (depression in the crystallization temperature, as well as the decrease in heat of melting and in the degree of crystallinity), and the processes of crystallite orientation in nanometre-sized volumes. In the first place, these anomalies are caused by radical changes in the balance between

nucleation and crystallite growth stages in confined volumes where formation of crystallites becomes easier, whereas their growth is restricted by a small (nanometre-sized) space. The comparative analysis of the effects of spatial restrictions on crystallization of polymers and low-molecular-mass compounds shows that the above listed changes in the thermodynamic characteristics are common to both high- and low-molecular-mass compounds.

The authors express their sincere appreciation to A V Efimov for fruitful discussions.

The review was prepared under financial support of the Russian Foundation for Basic Research (Project Nos 12-03-00617-a, 12-03-00338-a) and the Council on Grants at President of the Russian Federation (Programme of State Support for Leading Scientific Schools of the Russian Federation, Grant NSh-1683.2014.3).

References

1. M D Soucek, Z Zong, A J Johnson *JCT Res.* **3** 133 (2006)
2. D D Dlott *Mater. Sci. Technol.* **22** 463 (2006)
3. K Friedrich *J. Mater. Sci.* **33** 5535 (1998)
4. I P Suzdalev *Nanotekhnologiya. Fizikokhimiya Nanoklasterov, Nanostruktur i Nanomaterialov* (Nanotechnology. Physical Chemistry of Nanoclusters, Nanostructures and Nanomaterials) (Moscow: KomKniga, 2006)
5. S S Ivanchev, A N Ozerin *Polym. Sci., Ser. B* **48** 213 (2006) [*Vysokomol. Soedin., Ser. B* **48** 1531 (2006)]
6. R Qiao, H Deng, K W Putz, L C Brinson *J. Polym. Sci., Part B: Polym. Phys.* **49** 740 (2011)
7. A L Volynskii, N F Bakeev *Polym. Sci., Ser. C* **53** 35 (2011) [*Vysokomol. Soedin., Ser. C* **53** 1203 (2011)]
8. M Steinhart, S Senz, R B Wehrspohn, U Gosele, J H Wendorff *Macromolecules* **36** 3646 (2003)
9. M Steinhart, P Goring, H Dernaika, M Prabhukaran, U Gosele, E Hempel, T Thurn-Albrecht *Phys. Rev. Lett.* **97** 027801 (2006)
10. J Martin, J Maiz, J Sacristan, C Mijangos *Polymer* **53** 1149 (2012)
11. H Wu, W Wang, Y Huang, C Wang, Z Su *Macromolecules* **41** 7755 (2008)
12. K Shin, E Woo, Y G Jeong, C Kim, J Huh, K-W Kim *Macromolecules* **40** 6617 (2007)
13. Z Hu, G Baralia, V Bayot, J-F Gohy, A M Jonas *Nano Lett.* **5** 1738 (2005)
14. Y Liu, L Cui, F Guan, Y Gao, N E Hedin, L Zhu, H Fong *Macromolecules* **40** 6283 (2007)
15. C R Martin *Acc. Chem. Res.* **28** 61 (1995)
16. J Jang *Adv. Polym. Sci.* **199** 189 (2006)
17. A Arinstein, E Zussman *J. Polym. Sci., Part B: Polym. Phys.* **49** 691 (2011)
18. D Liang, B S Hsiao, B Chu *Adv. Drug Deliv. Rev.* **59** 1392 (2007)
19. C P Barnes, S A Sell, E D Boland, D G Simpson, G L Bowlin *Adv. Drug Deliv. Rev.* **59** 1413 (2007)
20. G B McKenna *Eur. Phys. J. Spec. Top.* **189** 285 (2010)
21. E A Shchukin, A V Pertsov, E A Amelina *Kolloidnaya Khimiya* (Colloid Chemistry) (Moscow: Vysshaya Shkola, 2004)
22. S S Voyutskii *Kurs Kolloidnoi Khimii* (Course of Colloid Chemistry) (Moscow: Khimiya, 1975)
23. J L Keddie, R A L Jones, R A Cory *Europhys. Lett.* **27** 59 (1994)
24. I M Ward, J Sweeney *An Introduction to the Mechanical Properties of Solid Polymers* (Chichester: Wiley, 2004)
25. J S Sharpl, J H Teichroeb, J A Forrest *Eur. Phys. J., E* **15** 473 (2004)
26. A D Schwab, D M G Agra, J-H Kim, S Kumar, A Dhinojwala *Macromolecules* **33** 4903 (2000)
27. J A Forrest, C Svanberg, K Revesz, M Rodahl, L M Torell, B Kasemo *Phys. Rev. E* **58** 1226 (1998)
28. O Wolff, D Johannsmann *J. Appl. Phys.* **87** 4182 (2000)
29. Y P Yampolsky *Russ. Chem. Rev.* **76** 59 (2007)
30. H Cao, J-P Yuan, R Zhang, C S Sundar, Y C Jean, R Suzuki, T Ohdaira, B Nielsen *Appl. Surf. Sci.* **149** 116 (1999)
31. L Xie, G B DeMaggio, W E Frieze, J DeVries, D W Gidley, H A Hristov, A F Yee *Phys. Rev. Lett.* **74** 4947 (1995)
32. Y C Jean, H Cao, G H Dai, R Suzuki, T Ohdaira, Y Kobayashi, K Hirata *Appl. Surf. Sci.* **116** 251 (1997)
33. J D Ferry *Viscoelastic Properties of Polymers* (New York: Wiley, 1961)
34. J Hyun, D E Aspenes, J J Cuomo *Macromolecules* **34** 2396 (2001)
35. M Alcoutlabi, G B McKenna *J. Phys.: Condens. Matter* **17** 461 (2005)
36. C J Ellison, J M Torkelson *Nat. Mater.* **2** 695 (2003)
37. C J Ellison, J M Torkelson *J. Polym. Sci., Part B: Polym. Phys.* **40** 2745 (2002)
38. C J Ellison, S D Kim, D B Hall, J M Torkrlson *Eur. Phys. J., E* **8** 155 (2002)
39. T Kajiyama, K Tanaka, A Takahara *Polymer* **39** 4665 (1998)
40. T Kajiyama, K Tanaka, A Takahara *Macromolecules* **30** 280 (1997)
41. T Kajiyama, K Tanaka, N Satomi, A Takahara *Sci. Technol. Adv. Mater.* **1** 31 (2000)
42. J H Kim, J Jang, D-Y Lee, W-C Zin *Macromolecules* **35** 311 (2002)
43. R M Overney, C Buenviaje, R Luginbuhl, F Dinelli *J. Therm. Anal. Cal.* **59** 205 (2000)
44. C Bollinne, V W Stone, V Carlier, A M Jonas *Macromolecules* **32** 4719 (1999)
45. B Frank, A P Gast, T R Russel, H R Brown, C Hawker *Macromolecules* **29** 6531 (1996)
46. X Zheng, B B Sauer, J G V Alsten, S A Schwartz, M H Rafailovich, J Sokolov, M Rubinstein *Phys. Rev. Lett.* **74** 407 (1995)
47. J A Forrest, K Dalnoki-Veress, J R Dutcher *Phys. Rev. E* **56** 5705 (1997)
48. D J Pochan, E K Lin, S K Satija, W-L Wu *Macromolecules* **34** 3041 (2001)
49. D S Fryer, R D Peters, E J Kim, J E Tomaszewski, J J de Pablo, P F Nealey, C C White, W-L Wu *Macromolecules* **34** 5627 (2001)
50. J Wang, M Tolan, O H Seeck, S K Sinha, O Bahr, M H Rafailovich, J Sokolov *Phys. Rev. Lett.* **83** 564 (1999)
51. A Lee, L Hamon, Y Holl, Y Grohens *Langmuir* **17** 7664 (2001)
52. L Hartmann, W Gorbatschow, J Hauwede, F Kremer *Eur. Phys. J., E* **8** 145 (2002)
53. J Baschnagel, F Varnik *J. Phys.: Condens. Matter* **17** 851 (2005)
54. P Scheidler, W Kob, K Binder *J. Phys. Chem. B* **108** 6673 (2004)
55. P Scheidler, W Kob, K Binder *Europhys. Lett.* **59** 701 (2002)
56. G D Smith, D Bedrov, O Borodin *Phys. Rev. Lett.* **90** 226103 (2003)
57. C E Porter, F D Blum *Macromolecules* **33** 7016 (2000)
58. J A Forrest, K Dalnoki-Veress, J R Stevens, J R Dutcher *Phys. Rev. Lett.* **77** 2002 (1996)
59. J A Forrest, K Dalnoki-Veress *Adv. Colloid Interface Sci.* **94** 167 (2001)
60. C M Stafford, S Guo, C Harrison, M Y M Chiang *Rev. Sci. Instrum.* **76** 062207 (2005)
61. C M Stafford, B D Vogt, C Harrison, D Julthongpiput, R Huang *Macromolecules* **39** 5095 (2006)
62. C M Stafford, C Harrison, K L Beers, A Karim, E J Amis, R Vanlandingham, H C Kim, W Volksen, R D Miller, E E Simonyi *Nat. Mater.* **3** 545 (2004)
63. R Huang, C M Stafford, B D Vogt *J. Aerosp. Eng.* **20** 38 (2007)
64. N Bowden, S Brittain, A G Evans, J W Hutchinson, G M Whitesides *Nature (London)* **393** 146 (1998)

65. A L Volynskii, S Bazhenov, O V Lebedeva, N F Bakeev *J. Mater. Sci.* **35** 547 (2000)
66. G Xu, W L Mattice *J. Chem. Phys.* **118** 5241 (2003)
67. T R Bohme, J de Pablo *J. Chem. Phys.* **116** 9939 (2002)
68. J A Torres, P F Nealey, J J de Pablo *Phys. Rev. Lett.* **85** 3221 (2000)
69. A R C Baljon, M H M van Weert, R Barber DeGraaf, R R Khare *Macromolecules* **38** 2391 (2005)
70. C Zhang, Y Guo, R D Priestle *J. Polym. Sci., Part B: Polym. Phys.* **51** 574 (2013)
71. V G Rostiashvili, V I Irzhak, B A Rozenberg *Steklovanie Polimerov* (Glass Transition of Polymers) (Leningrad: Khimiya, 1987)
72. B Jerome, J Commandeur *Nature (London)* **386** 589 (1997)
73. J H Rouse, P L Twaddle, G S Ferguson *Macromolecules* **32** 1665 (1999)
74. D S Fryer, P F Nealey, J de Pablo *Macromolecules* **33** 6439 (2000)
75. K L Ngai, A K Rizos, D J Plazek *J. Non-Cryst. Solids* **235 – 237** 435 (1998)
76. T S Jain, J de Pablo *Macromolecules* **35** 2167 (2002)
77. P Doruker, W L Mattice *Macromolecules* **32** 194 (1999)
78. P G de Geness *Eur. Phys. J., E* **2** 201 (2000)
79. T G Fox, P J Flory *J. Polym. Sci., Part B: Polym. Phys.* **14** 315 (1954)
80. N Satomi, K Tanaka, A Takahara, T Kajiyama, T Ishizone, S Nakahama *Macromolecules* **34** 8761 (2001)
81. P G Santagelo, C M Roland *Macromolecules* **31** 4581 (1998)
82. J A Forrest, J Mattsson *Phys. Rev. E* **61** R53 (2000)
83. K Fukao, Y Miyamoto *Phys. Rev. E* **61** 1743 (2000)
84. J H Kim, J Jang, W-C Zin *Langmuir* **16** 4064 (2000)
85. D V Lebedev, E M Ivan'kova, V A Marikhin, L P Myasnikova, V Seydewitz *Phys. Solid State* **51** 1744 (2009) [*Fiz. Tv. Tela* **51** 1645 (2009)]
86. R P Kambour *J. Polym. Sci., Macromol. Rev.* **7** 1 (1973)
87. E Passaglia *J. Phys. Chem. Solids* **48** 1075 (1987)
88. A L Volynskii, N F Bakeev *Solvent Crazing of Polymers* (Amsterdam, New York: Elsevier, 1996)
89. R P Kambour, R W Kopp *J. Polym. Sci., Part B: Polym. Phys.* **7** 183 (1969)
90. A L Volynskii, A Y Yarysheva, E G Rukhlya, A V Efimov, L M Yarysheva, N F Bakeev *Russ. Chem. Rev.* **82** 998 (2013)
91. H Masuda, K Fukuda *Science* **268** 1466 (1995)
92. G Sauer, G Brehm, S Schneider, K Nielsch, R B Wehrspohn, J Choi, H Hofmeister, U Gosele *J. Appl. Phys.* **91** 3243 (2002)
93. H Wu, W Wang, H Yang, Z Su *Macromolecules* **40** 4244 (2007)
94. R L Jones, S K Kumar, D L Ho, R M Briber, T P Russel *Nature (London)* **400** 146 (1999)
95. G Yu, W Cho, K Shin, in *Adsorption and Phase Behaviour in Nanochannels and Nanotubes* (Eds L J Dunne, G Manos) (London, New York: Springer, 2009) p. 101
96. K Shin, S Obukhov, J-T Chen, J Huh, Y Hwang, S Mok, P Dobriyal, P Thiyagarajan, T P Russell *Nat. Mater.* **6** 961 (2007)
97. C J G Plummer, A M Donald *Macromolecules* **23** 3929 (1990)
98. H Z Y Han, C B T McLeish, R A Duckett, N J Ward, A F Johnson, A M Donald, M Butler *Macromolecules* **31** 1348 (1998)
99. C J G Plummer, A M Donald *J. Mater. Sci.* **24** 1399 (1989)
100. A M Donald, E J Kramer *Polymer* **23** 1183 (1982)
101. A M Donald, E J Kramer *J. Polym. Sci., Part B: Polym. Phys.* **20** 899 (1982)
102. E J Kramer *Adv. Polym. Sci.* **52 – 53** 116 (1983)
103. S Granick, in *Polymers in Confined Environment* (Berlin: Springer, 1999)
104. G Reiter *Phys. Rev. Lett.* **68** 75 (1992)
105. M Daoud, P G de Gennes *J. Phys. (Paris)* **85** 35 (1977)
106. F Brochard-Wyart, E Raphael *Macromolecules* **23** 2276 (1990)
107. G Guillot, L Leger, F Rondelez *Macromolecules* **18** 2531 (1985)
108. C N Satterfield, C K Colton, W H Pitcher *AIChE J.* **19** 628 (1973)
109. C K Colton, C N Satterfield, C J Lai *AIChE J.* **21** 289 (1975)
110. W Haller *Macromolecules* **10** 83 (1977)
111. R E Beck, S J Schultz *Biochim. Biophys. Acta* **255** 273 (1972)
112. S J Schultz, R Valentine, C Y Choi *J. Gen. Physiol.* **73** 49 (1976)
113. T D Long, D L Jacobs, J L Anderson *J. Membr. Sci.* **9** 13 (1981)
114. C N Satterfield, C K Colton, B de Turckheim, T M Copeland *AIChE J.* **24** 937 (1978)
115. D Cannell, F Rondelez *Macromolecules* **13** 1599 (1980)
116. T D Long, J L Anderson *J. Polym. Sci., Part B: Polym. Phys.* **22** 1261 (1984)
117. I Teraoka, K H Langley, F E Karasz *Macromolecules* **26** 287 (1993)
118. H Grull, R Shaulitch, R Yerushalmi-Rozen *Macromolecules* **34** 8315 (2001)
119. E G Rukhlya, E A Litmanovich, A I Dolinnyi, L M Yarysheva, A L Volynskii, N F Bakeev *Macromolecules* **44** 5262 (2011)
120. A L Volynskii, E G Rukhlya, L M Yarysheva, N F Bakeev *Dokl. Phys. Chem.* **447** 200 (2012) [*Dokl. Akad. Nauk* **447** 176 (2012)]
121. A Y Yarysheva, D V Bagrov, E G Rukhlya, L M Yarysheva, A L Volynskii, N F Bakeev *Polym. Sci., Ser. A* **54** 779 (2012) [*Vysokomol. Soedin., Ser. A* **54** 1507 (2012)]
122. L M Yarysheva, E G Rukhlya, A Y Yarysheva, A L Volynskii, N F Bakeev *Rev. J. Chem.* **2** 1 (2012) [*Obzor. Zh. Khim.* **2** 3 (2012)]
123. G J Fleer, S M Cohen, J M H M Scheutjens, T Cosgrove *Polymer at Interfaces* (London, New York: Chapman and Hall, 1993)
124. R B Pandey, A Milchev, K Binder *Macromolecules* **30** 1194 (1997)
125. M Aubouy, O Guiselin, E Raphael *Macromolecules* **29** 7261 (1996)
126. P G de Gennes *Scaling Concepts in Polymer Physics* (Ithaca, New York: Cornell University Press, 1979)
127. M Doi, S F Edwards *The Theory of Polymer Dynamics* (Oxford: Clarendon Press, 1986)
128. M Adam, M Delsanti *Macromolecules* **10** 1229 (1977)
129. T Cosgrove, J M Sutherland *Polymer* **24** 534 (1983)
130. W Brown, P Zhou *Macromolecules* **24** 5151 (1991)
131. C L Bon, T Nicolai, M E Kuil, J G Hollander *J. Phys. Chem. B* **103** 10294 (1999)
132. T Kanematsu, T Sato, Y Imai, K Ute, T Kitayama *Polym J.* **37** 65 (2005)
133. Y-J Shenga, M-C Wang *J. Chem. Phys.* **114** 4724 (2001)
134. E F Casassa *J. Polym. Sci., Part B: Polym. Phys.* **5** 773 (1967)
135. S Daoudi, F Brochard *Macromolecules* **11** 751 (1978)
136. S Buttersack, H Rudolph, J Mahrholz, K Buchholz *Langmuir* **12** 3101 (1996)
137. N Tian, W Zhou, K Cui, Y Liu, Y Fang, X Wang, L Liu, L Li *Macromolecules* **44** 7704 (2011)
138. L Mandelkern *Crystallization of Polymers* (New York: McGraw-Hill, 1964)
139. S I Moon, T J McCarthy *Macromolecules* **36** 4253 (2003)
140. S Ai, G Lu, Q He, J Li *J. Am. Chem. Soc.* **125** 11140 (2003)
141. Z Liang, A S Susha, A Yu, F Caruso *Adv. Mater.* **15** 1849 (2003)
142. M Zhang, P Dobriyal, J-T Chen, T P Russell, J Olmo, A Merry *Nano Lett.* **6** 1075 (2006)
143. C R Martin *Science* **266** 1961 (1994)
144. J C Hulteen, C R Martin *J. Mater. Chem.* **7** 1075 (1997)

145. M Steinhart, J H Wendorff, A Greiner, R B Wehrspohn, K Nielsch, J Schilling, J Choi, U Gosele *Science* **296** 1997 (2002)
146. M Steinhart, R B Wehrspohn, U Gosele, J H Wendorff *Angew. Chem., Int. Ed.* **43** 1334 (2004)
147. V M Cepak, C R Martin *Chem. Mater.* **11** 1363 (1999)
148. V P Menon, J Lei, C R Martin *Chem. Mater.* **8** 2382 (1996)
149. J Maiz, J Martin, C Mijangos *Langmuir* **28** 12296 (2012)
150. H Wu, W Wang, Y Huang, Z Su *Macromol. Rapid Commun.* **30** 194 (2009)
151. R M Michell, A T Lorenzo, A J Muller, M-C Lin, H-L Chen, I Blaszczyk-Lezak, J Martin, C Mijangos *Macromolecules* **45** 1517 (2012)
152. E Woo, J Huh, Y G Jeong, K Shin *Phys. Rev. Lett.* **98** 136103 (2007)
153. A Henschel, P Huber, K Knorr *Phys. Rev. E* **77** 042602 (2008)
154. K Lee, G Yu, E Woo, S Hwang, K Shin, in *Adsorption and Phase Behaviour in Nanochannels and Nanotubes* (Eds L J Dunne, G Manos) (London, New York: Springer, 2009) p. 257
155. R L Cormia, F P Price, D Turnbull *J. Chem. Phys.* **37** 1333 (1962)
156. J R Burns, D Turnbull *J. Appl. Phys.* **37** 4021 (1966)
157. K Landfester *Adv. Mater.* **13** 765 (2001)
158. M Antonietti, K Landfester *Prog. Polym. Sci.* **27** 689 (2002)
159. B Vonnegut *J. Colloid Sci.* **3** 563 (1948)
160. K F Kelton *Solid State Phys.* **45** 75 (1991)
161. A Taden, K Landfester *Macromolecules* **36** 4037 (2003)
162. E Baer, A Hiltner, H D Keith *Science* **235** 1015 (1987)
163. J Kerns, A Hsieh, A Hiltner, E Baer *Macromol. Symp.* **147** 15 (1999)
164. J Kerns, A Hsieh, A Hiltner, E Baer *J. Appl. Polym. Sci.* **77** 1545 (2000)
165. V Ronesi, Y W Cheung, A Hiltner, E Baer *J. Appl. Polym. Sci.* **89** 153 (2003)
166. B C Poon, S P Chum, A Hiltner, E Baer *J. Appl. Polym. Sci.* **92** 109 (2004)
167. B C Poon, S P Chum, A Hiltner, E Baer *Polymer* **45** 893 (2004)
168. R Y F Liu, Y Jin, A Hiltner, E Baer *Macromol. Rapid Commun.* **24** 943 (2003)
169. H Wang, J K Keum, A Hiltner, E Baer *Macromolecules* **42** 7055 (2009)
170. H Wang, J K Keum, A Hiltner, E Baer *Macromolecules* **43** 3359 (2010)
171. J H Kim, J Jang, W Zin *Macromol. Rapid Commun.* **22** 386 (2001)
172. Y Wang, S Ge, M Rafailovich, J Sokolov, Y Zou, H Ade, J Luening, A Lustiger, G Maron *Macromolecules* **37** 3319 (2004)
173. H Schonherr, L E Bailey, C W Frank *Langmuir* **18** 490 (2002)
174. H Schonherr, C W Frank *Macromolecules* **36** 1199 (2003)
175. M V Massa, K Dalnoki-Veress, J A Forrest *Eur. Phys. J., E* **11** 191 (2003)
176. G Reiter, in *Soft Matter Characterization* (Eds R Borsali, R Pecora) (Berlin, Neidelberg: Springer, 2008) p. 1243
177. J S Langer *Rev. Mod. Phys.* **52** 1 (1980)
178. M Alexandre, P Dubois *Mater. Sci. Eng., Ser. R* **28** 1 (2000)
179. D Schmidt, D Shah, E P Giannelis *Curr. Opin. Solid State Mater. Sci.* **6** 205 (2002)
180. S S Ray, M Okamoto *Prog. Polym. Sci.* **28** 1539 (2003)
181. H Fischer *Mater. Sci. Eng., Ser. C* **23** 763 (2003)
182. A Usuki, N Hasegawa, M Kato *Adv. Polym. Sci.* **179** 135 (2005)
183. A Okada, A Usuki *Macromol. Mater. Eng.* **291** 1449 (2006)
184. K Chrissopoulou, K S Andrikopoulos, S Fotiadou, S Bollas, C Karageorgaki, D Christofilos, G A Voyiatzis, S H Anastasiadis *Macromolecules* **44** 9710 (2011)
185. S A Vshivkov, E V Rusinova *Fazovye Perekhody v Polimernykh Sistemakh, Vyzvannye Mekhanicheskim Polem* (Phase Transitions in Polymer Systems Induced by Mechanical Field) (Ekaterinburg: Ural Federal University, 2001)
186. *Orientatsionnye Yavleniya v Rastvorakh i Rasplavakh Polimerov* (Orientation Effects in Polymer Solutions and Melts) (Eds A Ya Malkin, S P Papkov) (Moscow: Khimiya, 1980)
187. E V Rusinova, S A Vshivkov, I V Zarudko, A L Nadol'skii *Polym. Sci., Ser. A* **39** 1074 (1997) [*Vysokomol. Soedin., Ser. A* **39** 1611 (1997)]
188. S A Vshivkov, E V Rusinova *Polym. Sci., Ser. A* **41** 445 (1999) [*Vysokomol. Soedin., Ser. A* **41** 662 (1999)]
189. E V Rusinova, S A Vshivkov *Polym. Sci., Ser. A* **39** 1066 (1997) [*Vysokomol. Soedin., Ser. A* **39** 1602 (1997)]
190. A J Pennings *J. Phys. Chem. Solids* **28** 389 (1967)
191. A J Pennings, A M Kiel *Kolloid Z.Z. Polym.* **205** 160 (1965)
192. A J Pennings, J M A A Mark, H C Booij *Kolloid Z.Z. Polym.* **236** 99 (1970)
193. D Blundell, A Keller, A J Kovacs *J. Polym. Sci., Part B: Polym. Phys.* **4** 481 (1966)
194. A Ya Malkin, V G Kulichikhin *Kolloid. Zh.* **41** 141 (1979) [a]
195. H Janeschitz-Kriegl, E Ratajski, M Stadlbauer *Rheol. Acta* **42** 355 (2003)
196. G Kumaraswamy, J A Kornfield, F Yeh, B S Hsiao *Macromolecules* **35** 1762 (2002)
197. Y Hayashi, G Matsuba, Y Zhao, K Nishida, T Kanaya *Polymer* **50** 2095 (2009)
198. R H Somani, L Yang, B S Hsiao, T Sun, N V Pogodina, A Lustiger *Macromolecules* **38** 1244 (2005)
199. G Kumaraswamy, A M Issaian, J A Kornfield *Macromolecules* **32** 7537 (1999)
200. P Panine, E di Cola, M Sztucki, T Narayanan *Polymer* **49** 676 (2008)
201. H Wu, W Wang, Z Su *Acta Polym. Sin.* **1** 425 (2009)
202. W Liang, C R Martin *J. Am. Chem. Soc.* **112** 9666 (1990)
203. Z Cai, J Lei, W Liang, V Menon, C R Martin *Chem. Mater.* **3** 960 (1991)
204. A L Volynskii, T E Grokhovskaya, G M Lukovkin, Yu K Godovskii, N F Bakeev *Vysokomol. Soedin., Ser. A* **26** 1456 (1984) [b]
205. A I Kitaigorodskii *Molekulyarnye Kristally* (Molecular Crystals) (Moscow: Nauka, 1971)
206. A L Volynskii, N F Bakeev *Strukturnaya Samoorganizatsiya Amorfnykh Polimerov* (Structural Self-Organization of Amorphous Polymers) (Moscow: Fizmatlit, 2005)
207. A Sharpless *Introduction to Polymer Crystallization* (London, Edward Arnold Publ., 1966)
208. A V Volkov, M A Moscvina, O V Arzhakova, A L Volynskii, N F Bakeev *J. Therm. Anal.* **38** 1311 (1992)
209. A L Volynskii, T E Grokhovskaya, N A Shitov, N F Bakeev *Vysokomol. Soedin., Ser. B* **22** 483 (1980) [b]
210. A L Volynskii, N A Shitov, A S Chegolya, N F Bakeev *Vysokomol. Soedin., Ser. B* **25** 393 (1983) [b]
211. A V Shubnikov *Epitaksiya. Fizicheskii Entsiklopedicheskii Slovar'* (Epitaxy. Physical Encyclopaedia) (Moscow: Sov. Entsiklopediya, 1966)

[a] — *Colloid J. (Engl. Transl.)*
[b] — *Polym. Sci. (Engl. Transl.)*